

Supporting Information

Intramolecular benzoallene–alkyne cycloaddition initiated by site-selective S_N2' reaction of epoxytetracene en route to π-extended pyracylene

Kei Kitamura,^{1,2} Kenta Asahina,¹ Kazuhiko Adachi,¹ and Toshiyuki Hamura*¹

¹*Department of Applied Chemistry for Environment, School of Science and Technology, Kwansei Gakuin University, 2-1 Gakuen, Sanda, Hyogo 669-1337, Japan*

²*Present Address: Faculty of Pharmaceutical Sciences, Tokushima Bunri University, 180 Yamashiro-cho, Tokushima 770-8514, Japan*

Table of Contents

1. General
2. Synthesis of epoxytetracene
3. Lewis acid-promoted cascade reaction of epoxytetracene
4. Synthesis of halogenated benzoindenotetracenes
5. Suzuki–Miyaura cross coupling of halogenated benzoindenotetracenes
6. Synthesis of π-extended pyracylenes
7. UV–Vis absorption spectra
8. Cyclic voltammograms
9. X-ray crystallographic data
10. NMR spectra
11. Theoretical calculations
12. References

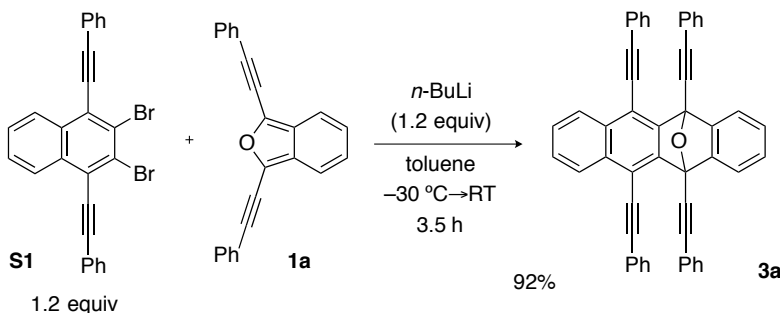
1. General

All experiments dealing with air- and moisture-sensitive compounds were conducted under an atmosphere of dry argon. THF (anhydrous; Wako Pure Chemical Industries, Ltd.) and toluene (anhydrous; Wako Pure Chemical Industries, Ltd.) were used as received.

For thin-layer chromatography (TLC) analysis, Merck pre-coated plates (silica gel 60 F₂₅₄, Art 5715, 0.25 mm) were used. For flash column chromatography, silica gel 60 N (spherical, neutral, 63–210 µm) from Kanto Chemical was used. Silica gel preparative TLC (PTLC) was performed on Merck silica gel 60 PF₂₅₄ (Art 7749).

¹H NMR and ¹³C NMR were measured on a JEOL JNM ECA-300 and a JEOL JNM ECX-500II spectrometer. Attenuated Total Reflectance Fourier Transformation Infrared (ATR-FTIR) spectra were recorded on a JASCO FT/IR-4200 infrared spectrometer. UV-VIS spectra were recorded on a JASCO V-630 spectrophotometer. High resolution mass spectra were obtained with a JEOL The AccuTOF LC-plus JMS-T100LP and Bruker micrOTOF. Cyclic voltammetry (CV) were recorded on a ALS/CH Instruments Electrochemical Analyzer Model 620D. Melting points (Mp) were measured on an OptiMelt Automated Melting Point System from Stanford research systems and are uncorrected. Preparative gel permeation chromatography (GPC) was performed on a recycling preparative HPLC (JAI LC-9225 NEXT equipped with JAIGEL-3H and JAIGEL-2.5H columns; Japan Analytical Industry Co. Ltd.).

2. Synthesis of epoxytetracene^[S1]



To a mixture of dibromonaphthalene **S1** (233 mg, 0.479 mmol) and isobenzofuran **1a** (127 mg, 0.399 mmol) in toluene (8.0 mL) was added *n*-BuLi (1.60 M in hexane, 0.30 mL, 0.48 mmol) at –30 °C. After gradual warming to room temperature for 3.5 h, the reaction was quenched by an addition of H₂O and the products were extracted with EtOAc (×3). The combined extracts were washed with brine, and dried over Na₂SO₄. Concentration and purification by silica-gel column chromatography (hexane/acetone = 95/5→80/20) afforded epoxytetracene **3a** (236 mg, 92%) as a light brown solid.

Mp 228 °C (dec);

R_f 0.28 (hexane/EtOAc = 9/1);

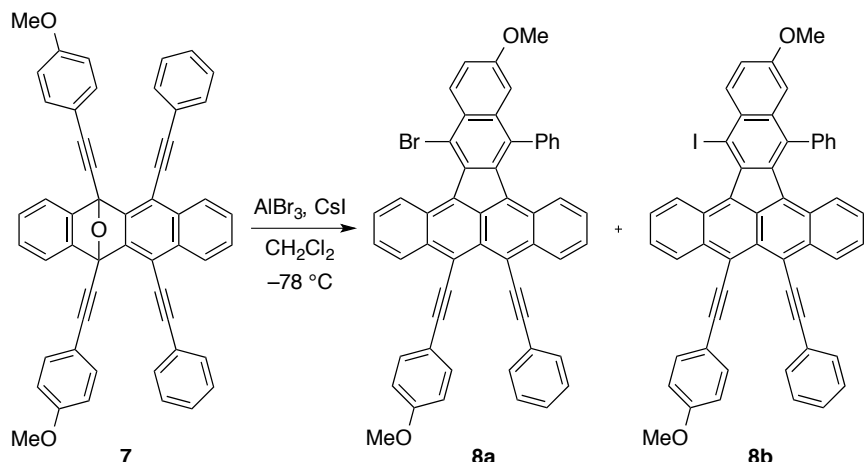
¹H NMR (CDCl₃, 500 MHz) 7.19–7.26 (m, 10H), 7.28–7.34 (m, 4H), 7.48–7.53 (m, 8H), 7.60–7.64 (m, 2H), 7.64–7.68 (m, 2H), 8.43–8.47 (m, 2H);

¹³C NMR (CDCl₃, 125 MHz) 81.1, 82.2, 83.3, 91.8, 101.1, 114.1, 120.3, 122.0, 123.0, 126.6, 127.4, 127.7, 128.1, 128.2, 128.6, 129.0, 131.8, 132.3, 132.5, 144.5, 147.2;

IR (ATR, cm^{−1}) 3055, 2245, 1599, 1490, 1442, 1373, 1322, 1170, 1069, 1025, 967, 925, 898, 749, 685;

HRMS (ESI) calcd for C₅₀H₂₉O [M+H]⁺ 645.2218; found 645.2230.

3. Lewis acid-promoted cascade reaction of epoxytetracene



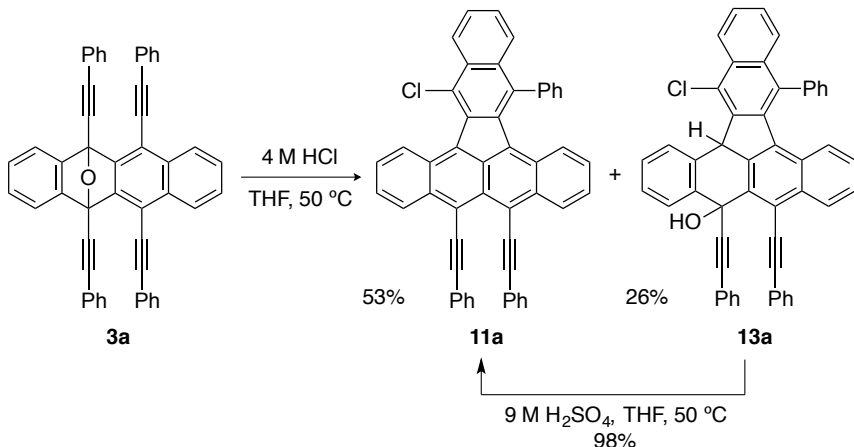
To a mixture of epoxytetracene **7** (141 mg, 0.200 mmol) and CsI (217 mg, 0.0835 mmol) in CH_2Cl_2 (10 mL) was added AlBr_3 (1.0 M in dibromomethane, 0.40 mL, 0.40 mmol) at -78°C . After 5 min, the reaction was stopped by adding sat. aq. NaHCO_3 . The mixture was filtered through Celite® pad, which was washed with CH_2Cl_2 . The products were extracted with CH_2Cl_2 ($\times 3$), and the combined extracts were washed with brine, dried (Na_2SO_4), and concentrated *in vacuo*. The residue was purified by silica-gel flash column chromatography (hexane/toluene = 40/60) to give products, which was further purified by PTLC (hexane/toluene = 30/70) and gel permeation chromatography (CHCl_3) to afford a mixture of bromo-benzoindenotetracene **8a** and iodo-benzoindenotetracene **8b** (2.6 mg) as dark green solids. Recrystallization of benzoindenotetracene **8** from benzene gave bromo-benzoindenotetracene **8a** as a green needle.

^1H NMR (CDCl_3 , 500 MHz) 3.81 (s), 3.82 (s), 6.72–6.79 (m), 7.21–7.37 (m), 7.45–7.64 (m), 8.44 (d, $J = 9.2$ Hz), 8.52–8.56 (m), 8.71–8.96 (m);

^{13}C NMR (CDCl_3 , 125 MHz) 55.3, 55.36, 55.42, 88.3, 89.3, 106.9, 107.5, 108.0, 113.8, 116.1, 117.6, 118.2, 118.4, 118.6, 119.4, 119.7, 123.9, 125.0, 125.1, 125.3, 125.5, 125.9, 126.0, 126.5, 126.6, 127.1, 127.77, 127.83, 128.13, 128.19, 128.22, 128.3, 128.6, 128.9, 129.2, 130.0, 121.7, 131.9, 132.2, 132.3, 133.2, 134.1, 134.7, 134.8, 135.0, 135.1, 135.4, 136.5, 136.7, 136.8, 138.0, 139.2, 139.7, 140.0, 140.1, 158.7, 159.7;

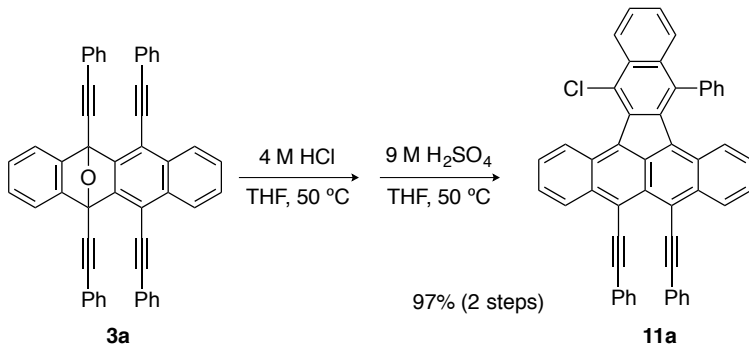
HRMS (MALDI, dithranol matrix) calcd for $\text{C}_{52}\text{H}_{31}\text{O}_2\text{Br}$ [M]⁺ 766.1502; found 766.1492, calcd for $\text{C}_{52}\text{H}_{31}\text{O}_2\text{I}$ [M]⁺ 814.1357; found 814.1363.

4. Synthesis of halogenated benzoindenotetracenes



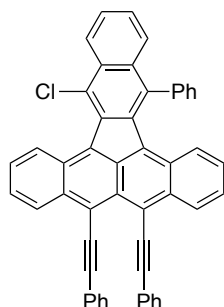
To a solution of epoxytetracene **3a** (308 mg, 0.478 mmol) in THF (4.8 mL) was added 4 M aqueous HCl (1.2 mL). After stirring at 50 °C for 10 h, the reaction was carefully quenched by an addition of sat. aq. NaHCO₃. The products were extracted with EtOAc ($\times 3$) and the combined extracts were washed by brine, and dried over Na₂SO₄. Concentration and purification by silica-gel column chromatography (hexane/acetone = 95/5) afforded chloro-benzoindenotetracene **11a** (158 mg, 53%) as a deep-blue solid and alcohol **13a** (87.9 mg, 26%) as colorless amorphous solid.

To a solution of alcohol **13a** (21.6 mg, 0.0317 mmol) in THF (1.6 mL) was added 9 M aqueous H₂SO₄ (0.4 mL). After stirring at 50 °C for 2 h, the reaction was carefully quenched by an addition of sat. aq. NaHCO₃. The products were extracted with EtOAc ($\times 3$) and the combined extracts were washed by brine, and dried over Na₂SO₄. Concentration and purification by silica-gel column chromatography (hexane/acetone = 9/1) afforded chloro-benzoindenotetracene **11a** (20.6 mg, 98%) as a deep-blue solid.



To a solution of epoxytetracene **3a** (27.0 mg, 0.0419 mmol) in THF (0.4 mL) was added 4 M aqueous HCl (0.1 mL). After stirring at 50 °C for 6 h, the reaction was carefully quenched by an addition of sat. aq. NaHCO₃. The products were extracted with EtOAc ($\times 3$) and the combined extracts were washed by brine, and dried over Na₂SO₄. After concentration, the residue was then dissolved in THF (1.6 mL). To the mixture was added 9 M aqueous H₂SO₄ (0.4 mL) and stirred at 50 °C for 3 h. After the completion of the reaction, the mixture was carefully quenched by an addition of sat. aq. NaHCO₃. The products were extracted with EtOAc ($\times 3$) and the combined extracts were washed by brine, and dried over Na₂SO₄. Concentration and purification by silica-gel column chromatography

(hexane/acetone = 9/1→8/2) afforded chloro-benzoindeno[1,2-*b*]tetracene **11a** (27.0 mg, 97%) as a deep-blue solid.



mp >300 °C;

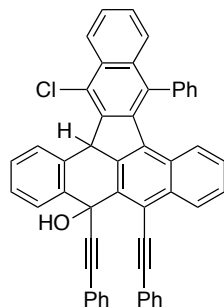
R_f 0.43 (hexane/acetone = 9/1);

^1H NMR (500 MHz, CDCl_3) 6.79 (ddd, 1H, J = 9.2, 6.3, 1.1 Hz), 7.18–7.35 (m, 8H), 7.48–7.68 (m, 13H), 7.99 (d, 1H, J = 8.6 Hz), 8.63 (d, 1H, J = 8.6 Hz), 8.82 (d, 1H, J = 8.6 Hz), 8.86 (d, 1H, J = 8.0 Hz), 8.98 (d, 1H, J = 8.0 Hz);

^{13}C NMR (125 MHz, CDCl_3) 89.2, 89.3, 107.0, 107.3, 119.3, 119.8, 123.8, 125.18, 125.24, 125.3, 125.9, 126.0, 126.1, 126.3, 126.4, 126.8, 127.0, 127.3, 127.7, 127.9, 128.0, 128.1, 128.21, 128.23, 128.27, 128.6, 129.1, 131.6, 131.7, 131.8, 132.2, 132.3, 133.3, 133.5, 134.7, 136.6, 136.8, 136.9, 138.4, 139.8;

IR (ATR, cm^{-1}) 3058, 2922, 2187, 1488, 1441, 1396, 1326, 1270, 1181, 1071, 1024, 948, 899, 862, 749, 687;

HRMS (MALDI, TCNQ matrix) m/z calcd for $\text{C}_{50}\text{H}_{27}\text{Cl} [\text{M}]^+$: 662.1796; found: 662.1809.



R_f 0.27 (hexane/acetone = 9/1);

^1H NMR (500 MHz, CDCl_3) 5.79 (s, 2H), 6.83–6.86 (m, 1H), 6.97 (d, 1H, J = 8.6 Hz), 7.21–7.42 (m, 10H), 7.44–7.78 (m, 11H), 7.98 (d, 1H, J = 8.6 Hz), 8.17 (d, 1H, J = 8.0, 1.2 Hz), 8.54–8.58 (m, 2H);

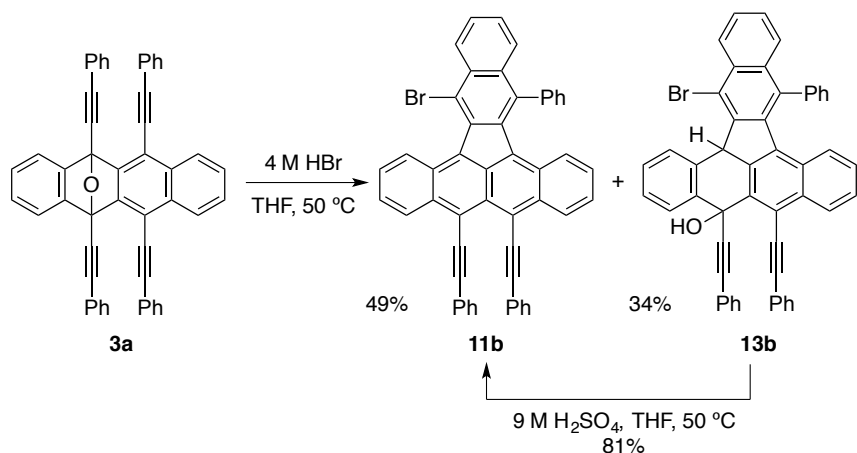
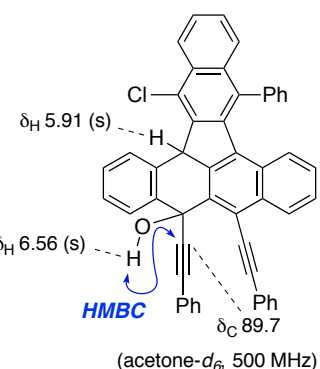
^1H NMR (500 MHz, acetone- d_6) 5.91 (s, 1H), 6.56 (s, 1H), 6.77–6.82 (m, 1H), 6.93–6.97 (m, 1H), 7.24–7.65 (m, 18H), 7.72–7.76 (m, 1H), 7.79–7.82 (m, 2H), 7.91 (d, 1H, J = 8.6 Hz), 8.20 (dd, 1H, J = 8.1, 1.2 Hz), 8.51 (d, 1H, J = 8.6 Hz), 8.69 (d, 1H, J = 8.6 Hz);

^{13}C NMR (125 MHz, CDCl_3) 48.5, 70.0, 83.4, 85.6, 88.6, 103.5, 115.4, 122.2, 122.3, 124.1, 124.3, 125.56, 125.6, 125.7, 126.3, 126.4, 126.7, 126.9, 127.1, 127.2, 127.6, 127.8, 128.1, 128.2, 128.5, 128.7, 128.8, 129.1, 129.3, 129.5, 130.3, 131.6, 131.9, 132.2, 132.6, 134.2, 134.5, 134.9, 139.28, 139.33, 140.0, 140.3, 142.3, 143.1;

^{13}C NMR (125 MHz, acetone- d_6) 49.4, 70.8, 83.8, 87.1, 89.7, 103.4, 117.7, 121.2, 123.0, 124.4, 124.6, 125.1, 126.2, 126.5, 126.8, 127.1, 127.4, 127.6, 127.95, 127.99, 128.3, 128.6, 129.3, 129.4, 129.5, 129.6, 129.7, 129.9, 130.0, 131.0, 132.39, 132.41, 132.8, 132.9, 133.2, 133.6, 134.6, 135.36, 135.42, 135.9, 140.3, 140.7, 140.96, 141.11, 144.4, 144.8;

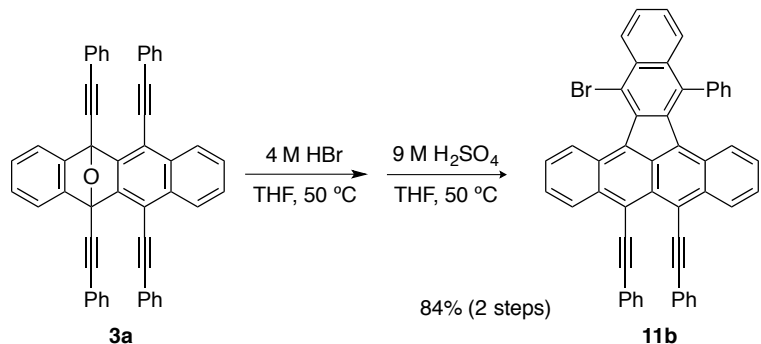
IR (ATR, cm^{-1}) 3437, 3065, 2204, 1706, 1598, 1490, 1354, 1219, 1119, 1067, 947, 751, 687, 654;

HRMS (ESI) m/z calcd for $C_{50}H_{28}ClO [M-H]^+$: 679.1834; found: 679.1858.

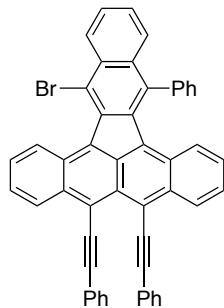


To a solution of epoxytetracene **3a** (26.1 mg, 0.0405 mmol) in THF (0.8 mL) was added 4 M aqueous HBr (0.2 mL). After stirring at 50 °C for 4 h, the reaction was carefully quenched by an addition of sat. aq. NaHCO₃. The products were extracted with EtOAc ($\times 3$) and the combined extracts were washed by brine, and dried over Na₂SO₄. Concentration and purification by preparative silica-gel column chromatography (hexane/acetone = 85/15) afforded bromo-benzoindenotetracene **11b** (14.1 mg, 49%) as a deep-blue solid and alcohol **13b** (10.0 mg, 34%) as colorless amorphous solid.

To a solution of alcohol **13b** (11.9 mg, 0.0164 mmol) in THF (1.6 mL) was added 9 M aqueous H₂SO₄ (0.4 mL). After stirring at 50 °C for 2 h, the reaction was carefully quenched by an addition of sat. aq. NaHCO₃. The products were extracted with EtOAc ($\times 3$) and the combined extracts were washed by brine, and dried over Na₂SO₄. Concentration and purification by silica-gel column chromatography (hexane/acetone = 9/1) afforded bromo-benzoindenotetracene **11b** (9.4 mg, 81%) as a deep-blue solid.



To a solution of epoxypentacene **3a** (256 mg, 0.397 mmol) in THF (9.0 mL) was added 4 M aqueous HBr (1.0 mL). After stirring at 50 °C for 4 h, the reaction was carefully quenched by an addition of sat. aq. NaHCO₃. The products were extracted with EtOAc ($\times 3$) and the combined extracts were washed by brine, and dried over Na₂SO₄. After concentration, the residue was then dissolved in THF (2.0 mL). To the mixture was added 9 M aqueous H₂SO₄ (0.5 mL) and stirred at 50 °C for 2 h. After completion of the reaction, the mixture was carefully quenched by an addition of sat. aq. NaHCO₃. The products were extracted with EtOAc ($\times 3$) and the combined extracts were washed by brine, and dried over Na₂SO₄. Concentration and purification by silica-gel column chromatography (hexane/acetone = 9/1) afforded bromo-benzoindeno-tetracene **11b** (235 mg, 84% over 2 steps) as a deep-blue solid.



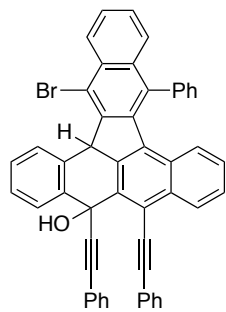
mp >300 °C;

R_f 0.41 (hexane/acetone = 9/1);

¹H NMR (500 MHz, CDCl₃) 6.77 (ddd, 1H, *J* = 1.2, 6.3, 8.6 Hz), 7.18–7.33 (m, 8H), 7.47–7.66 (m, 13H), 7.95 (d, 1H, *J* = 7.5 Hz), 8.63 (dd, 1H, *J* = 1.2, 8.6 Hz), 8.79 (d, 1H, *J* = 8.6 Hz), 8.80 (d, 1H, *J* = 8.6 Hz), 8.96 (d, 1H, *J* = 9.2 Hz);

¹³C NMR (125 MHz, CDCl₃) 89.2, 89.3, 107.0, 107.4, 117.7, 119.4, 119.8, 123.8, 125.2, 125.6, 126.0, 126.5, 126.8, 127.5, 127.7, 127.9, 128.07, 128.15, 128.25, 128.5, 128.9, 128.9, 129.1, 131.7, 131.8, 132.3, 132.5, 133.0, 133.4, 135.1, 136.6, 136.9, 139.0, 139.7, 139.8;

IR (ATR, cm⁻¹) 3060, 2924, 2184, 1596, 1490, 1442, 1398, 1324, 1264, 1177, 1028, 908, 754, 688;
HRMS (MALDI, TCNQ matrix) *m/z* calcd for C₅₀H₂₇Br [M]⁺: 706.1291; found: 706.1282.



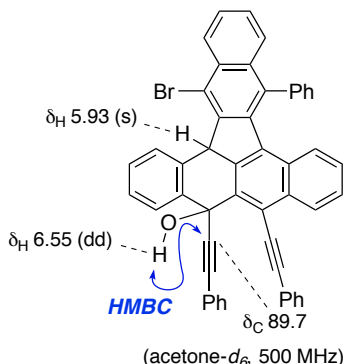
R_f 0.24 (hexane/acetone = 9/1);

^1H NMR (500 MHz, acetone- d_6) 5.93 (s, 1H), 6.55 (d, 1H, J = 1.7 Hz), 6.81–6.87 (m, 1H), 6.97–7.02 (m, 1H), 7.25–7.72 (m, 18H), 7.75–7.83 (m, 3H), 7.94 (dd, 1H, J = 8.0, 7.5 Hz), 8.19 (d, 1H, J = 8.0 Hz), 8.52–8.55 (m, 1H), 8.68–8.72 (m, 1H);

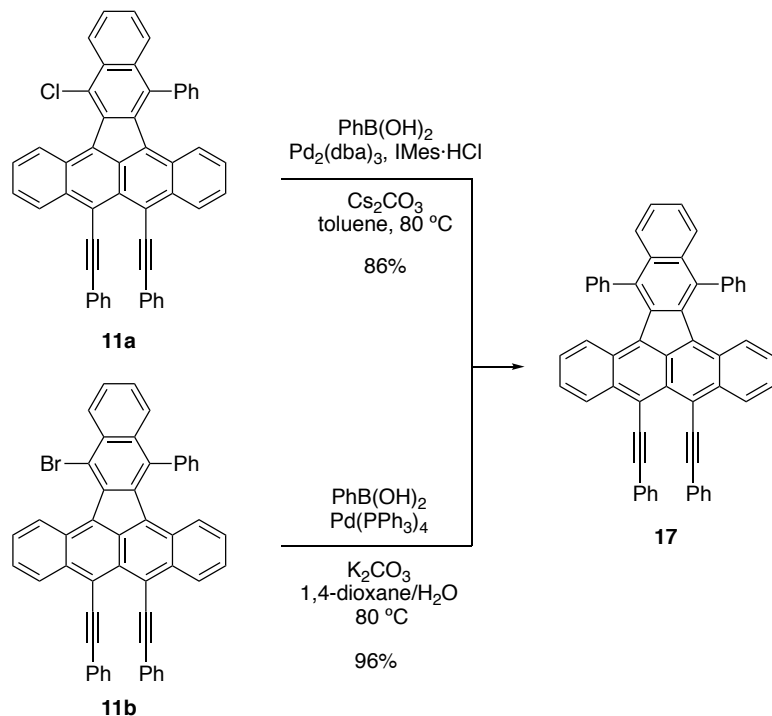
^{13}C NMR (125 MHz, acetone- d_6) 51.2, 70.9, 83.8, 87.1, 89.7, 103.4, 117.6, 122.3, 123.0, 124.4, 125.0, 125.2, 126.4, 126.5, 126.7, 126.8, 126.9, 127.1, 127.3, 127.45, 127.52, 127.7, 127.9, 128.4, 128.5, 129.3, 129.5, 129.7, 130.1, 132.2, 132.4, 132.7, 132.8, 133.0, 133.4, 134.6, 135.2, 135.9, 140.7, 140.9, 141.0, 142.9, 144.2, 144.9;

IR (ATR, cm^{-1}) 3516, 3064, 2246, 1597, 1490, 1442, 1322, 1121, 1068, 907, 754, 689;

HRMS (ESI) m/z calcd for $\text{C}_{50}\text{H}_{28}\text{BrO} [\text{M}-\text{H}]^-$: 723.1329; found: 723.1320.



5. Suzuki–Miyaura cross coupling of halogenated benzoindenotetracenes



To a mixture of chloro-benzoindenotetracene **11a** (17.1 mg, 0.0258 mmol), PhB(OH)_2 (11.0 mg, 0.0902 mmol), and Cs_2CO_3 (39.0 mg, 0.120 mmol) in 1,4-dioxane (1.5 mL) was added $\text{Pd}_2(\text{dba})_3 \cdot \text{CHCl}_3$ (3.1 mg, 2.99 μmol) and $\text{IMes}\cdot\text{HCl}$ (2.0 mg, 5.87 μmol). The mixture was evacuated and backfilled with argon ($\times 3$). After stirring at 80°C for 2 h, the mixture was filtered through Celite[®] pad. Purification by silica-gel column chromatography (hexane/ CH_2Cl_2 = 9/1 \rightarrow 8/2) afforded diphenyl-benzoindenotetracene **17** (15.6 mg, 86%) as a deep-green solid.

To a mixture of bromo-benzoindenotetracene **11b** (9.0 mg, 0.0127 mmol), PhB(OH)_2 (6.2 mg, 0.0508 mmol), and K_2CO_3 (14.0 mg, 0.101 mmol) in 1,4-dioxane (0.8 mL) and H_2O (0.2 mL) was added $\text{Pd}(\text{PPh}_3)_4$ (1.5 mg, 1.29 μmol). The mixture was evacuated and backfilled with argon ($\times 3$). After stirring at 80°C for 2 h, the mixture was filtered through Celite[®] pad. Purification by silica-gel column chromatography (hexane/acetone = 85/15) afforded diphenyl-benzoindenotetracene **17** (8.6 mg, 96%) as a deep-green solid.

mp >300 °C;

R_f 0.42 (hexane/acetone = 9/1);

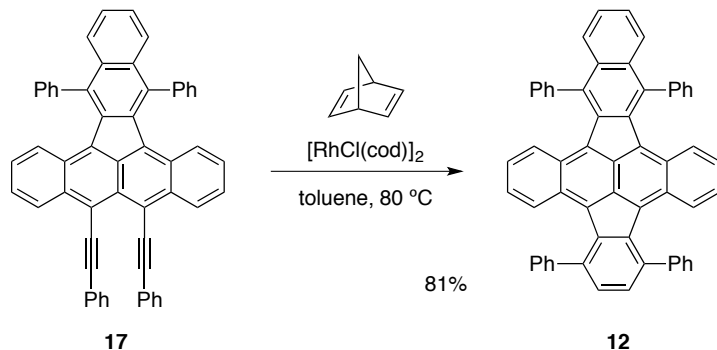
^1H NMR (500 MHz, CDCl_3) 6.80 (ddd, 2H, J = 9.2, 6.3, 1.1 Hz), 7.17–7.26 (m, 6H), 7.33 (ddd, 2H, J = 8.6, 6.3, 1.1 Hz), 7.44–7.53 (m, 14H), 7.64–7.66 (m, 4H), 8.09–8.12 (m, 2H), 8.80 (d, 2H, J = 8.6 Hz);

^{13}C NMR (125 MHz, CDCl_3) 89.4, 106.7, 118.6, 123.9, 124.8, 126.0, 126.1, 126.3, 126.4, 127.4, 127.5, 128.01, 128.07, 128.11, 129.0, 131.6, 132.5, 132.7, 133.3, 133.5, 135.3, 136.7, 137.9, 140.2;

IR (ATR, cm^{-1}) 3056, 2923, 2183, 1489, 1399, 1260, 1021, 799, 752, 688;

HRMS (MALDI, TCNQ matrix) m/z calcd for $\text{C}_{56}\text{H}_{33} [\text{M}+\text{H}]^+$: 705.2577; found: 705.2553.

6. Synthesis of π -Extended Pyracylenes



To a mixture diyne **17** (36.3 mg, 0.0515 mmol) and $[\text{Rh}(\text{cod})\text{Cl}]_2$ (2.5 mg, 5.1 μmol) in toluene (2.5 mL) was added freshly distilled 2,5-norbornadiene (100 μL , 0.985 mmol). The mixture was degassed by bubbling argon for 5 min and then stirred at 80 °C for 24 h. After cooling to room temperature and the mixture was directly purified by silica-gel column chromatography (CS_2) to give π -extended pyracylene **12** (30.6 mg, 81%) as dark green solid.

mp >300 °C;

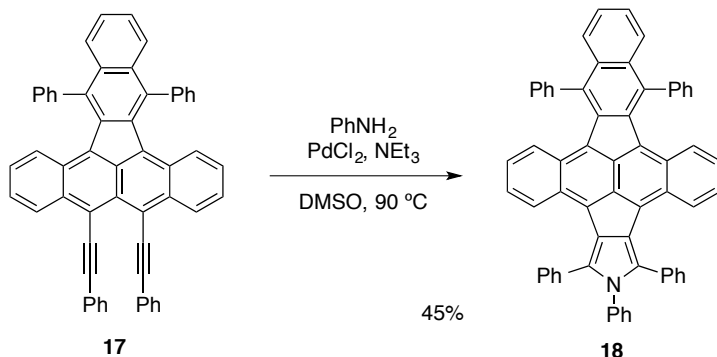
R_f 0.33 (hexane/ CH_2Cl_2 = 8/2);

^1H NMR (500 MHz, $\text{CS}_2/\text{CDCl}_3$ = 5/1) 6.40–6.45 (m, 4H), 6.90–6.94 (m, 4H), 7.24–7.40 (m, 10H), 7.42–7.47 (m, 2H), 7.49–7.54 (m, 8H), 7.59–7.62 (m, 4H), 7.71–7.75 (m, 2H);

^{13}C NMR could not be obtained due to the poor solubility in common organic solvents.

IR (ATR, cm^{-1}) 2921, 2851, 1731, 1575, 1464, 1377, 1260, 1073, 1023, 799, 761, 699;

HRMS (MALDI, DCTB matrix) m/z calcd for $\text{C}_{58}\text{H}_{34} [\text{M}]^+$: 730.2655; found: 730.2642.



A mixture of diyne **17** (25.5 mg, 0.036 mmol), aniline (16 μL , 0.18 mmol), NEt_3 (101 μL , 0.72 mmol), PdCl_2 (0.6 mg, 0.0036 mmol), DMSO (2.0 mL) was heated at 90 °C. After stirring for 8 h, the mixture was cooled at room temperature and diluted with CH_2Cl_2 and H_2O . The products were extracted with CH_2Cl_2 ($\times 3$) and the combined extracts were washed by brine, and dried over Na_2SO_4 . Concentration and purification by silica-gel column chromatography (hexane/ CH_2Cl_2 = 85/15) afforded pyrrole-fused π -extended pyracylene **18** (13.8 mg, 45%) as a dark green solid.

mp >300 °C;

R_f 0.43 (hexane/acetone = 8/2);

^1H NMR (500 MHz, CDCl_3) 6.52–6.56 (m, 2H), 6.62–6.65 (m, 2H), 6.96–7.01 (m, 4H), 7.08–7.16 (m, 4H), 7.28–7.34 (m, 9H), 7.41–7.55 (m, 10H), 7.66–7.68 (m, 4H), 7.81–7.84 (m, 2H);

¹³C NMR (125 MHz, CDCl₃) 112.5, 117.1, 123.7, 124.4, 125.7, 127.4, 127.8, 128.0, 128.29, 128.32, 128.8, 129.03, 129.07, 129.2, 129.3, 129.4, 129.5, 130.8, 130.9, 131.5, 131.8, 132.4, 133.05, 133.07, 133.1, 134.7, 138.4, 140.1, 141.1;

IR (ATR, cm⁻¹) 2923, 2851, 1716, 1558, 1488, 1443, 1362, 1261, 1074, 1025, 761, 700;
HRMS (MALDI, TCNQ matrix) *m/z* calcd for C₆₂H₃₇N [M]⁺: 795.2921; found: 795.2919.

7. UV–Vis Absorption Spectra

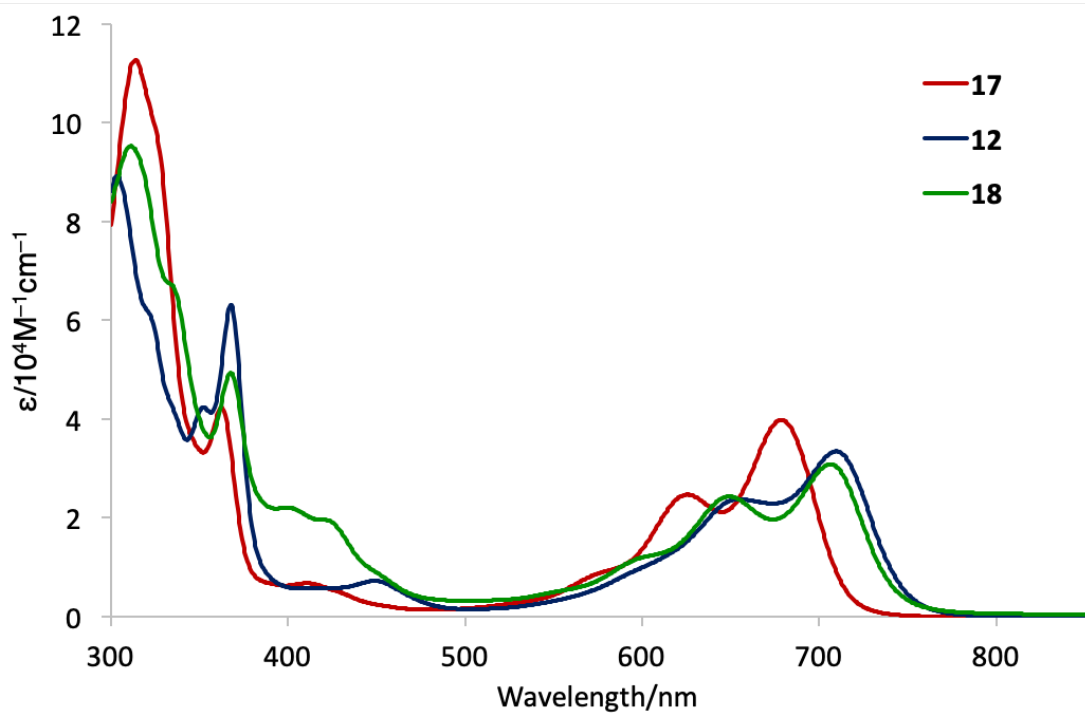


Figure S1. UV–Vis Absorption Spectra of **17** (red), **12** (blue), and **18** (green) in toluene (2×10^{-5} M).

compound	λ_{max} (nm)	$\log \epsilon$
17	679	4.60
12	710	4.52
18	707	4.49

8. Cyclic Voltammograms

The measurements were carried out in degassed THF (1.0 mM) with 0.1 M *n*-Bu₄NPF₆ as supporting electrolyte at room temperature. A glassy carbon was used as working electrode, platinum wire was used as counter electrode, and Ag/AgNO₃ was used as reference electrode. The scan rate is 100 mV/s. The potential was calibrated against the ferrocene/ferrocenium couple (Fc/Fc⁺).

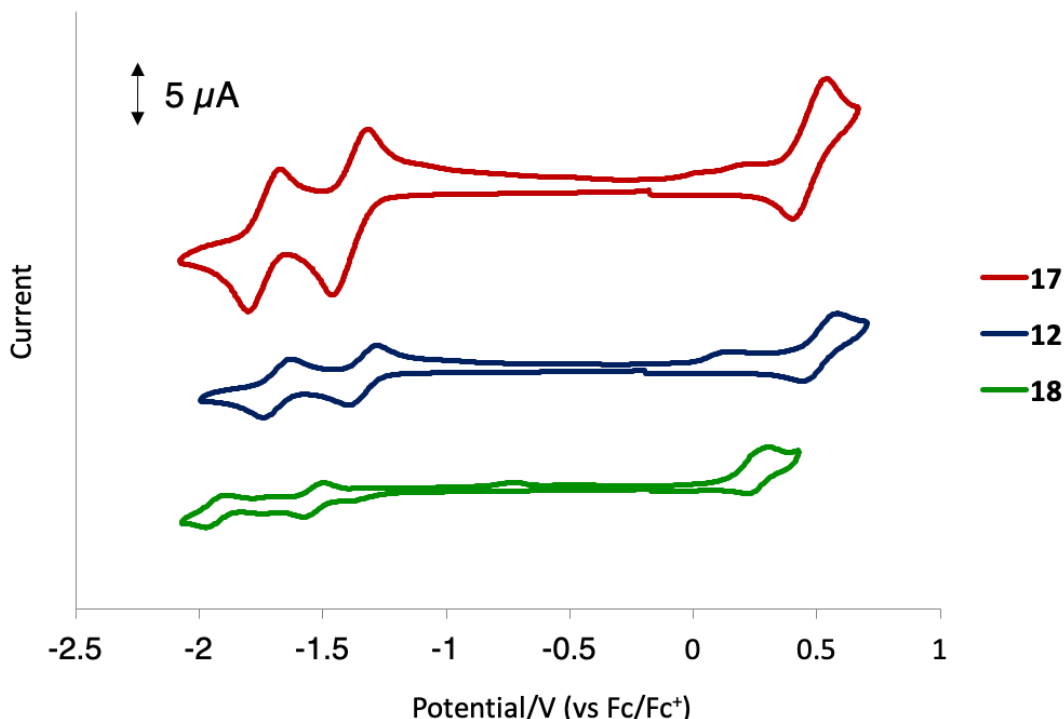


Figure S2. Cyclic voltammograms of **17** (red), **12** (blue), and **18** (green) in THF (1.0 mM).

compound	E ₁ ^{red} (V)	E ₂ ^{red} (V)	E ^{ox} (V)	E _g ^{elect} (V)	E _g ^{opt} (V) ^[1]	HOMO (eV) ^[2]	LUMO (eV) ^[3]
17	-1.39	-1.74	+0.34	1.73	1.73	-5.14	-3.41
12	-1.34	-1.68	+0.31	1.65	1.66	-5.11	-3.46
18	-1.54	-1.93	+0.15	1.69	1.67	-4.95	-3.26

[1] Estimated from the onset of the UV/Vis absorption spectrum by using E_g^{opt} = 1240/λ_{onset}. [2] E_{HOMO} = -(4.8 + E^{ox}) eV. [3] E_{LUMO} = -(4.8 + E₁^{red}) eV.

9. X-ray crystallographic data

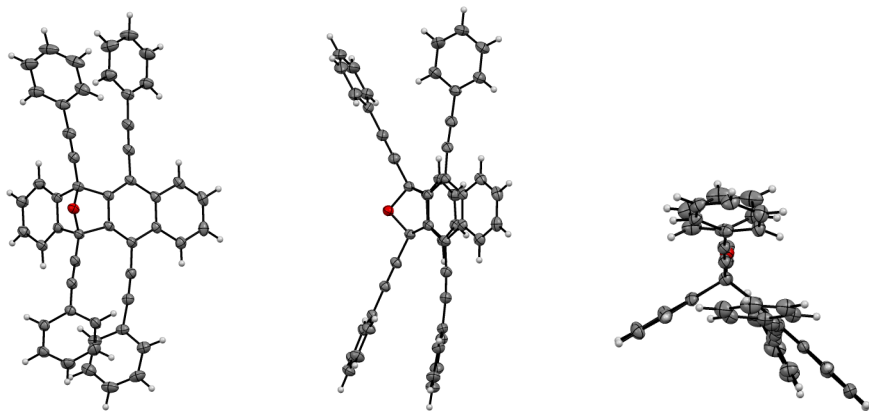


Figure S3. ORTEP drawings of **3a** at the 50% probability level (CCDC 1871871).

$C_{50}H_{28}O$, MW = 644.72, 0.50 x 0.20 x 0.20 mm, Triclinic, space group $P\bar{1}$, $Z = 2$, $T = 150(2)$ K, $a = 7.668(2)$ Å, $b = 14.882(4)$ Å, $c = 16.727(5)$ Å, $\alpha = 65.723(9)^\circ$, $\beta = 84.051(15)^\circ$, $\gamma = 77.710(14)^\circ$, $V = 1699.8(8)$ Å³, $\lambda(\text{Mo K}\alpha) = 0.71075$ Å, $\mu = 0.074$ mm⁻¹. Intensity data were collected on a Rigaku R-AXIS RAPID II. The structure was solved by direct methods (*SHELXS97*) and refined by the full-matrix least-squares on F^2 (*SHELXL-2014/7*). A total of 18845 reflections were measured and 7611 were independent. Final $R_1 = 0.0501$, $wR_2 = 0.1159$ (5978 refs; $I > 2\sigma(I)$), and GOF = 1.079 (for all data, $R_1 = 0.0664$, $wR_2 = 0.1271$).

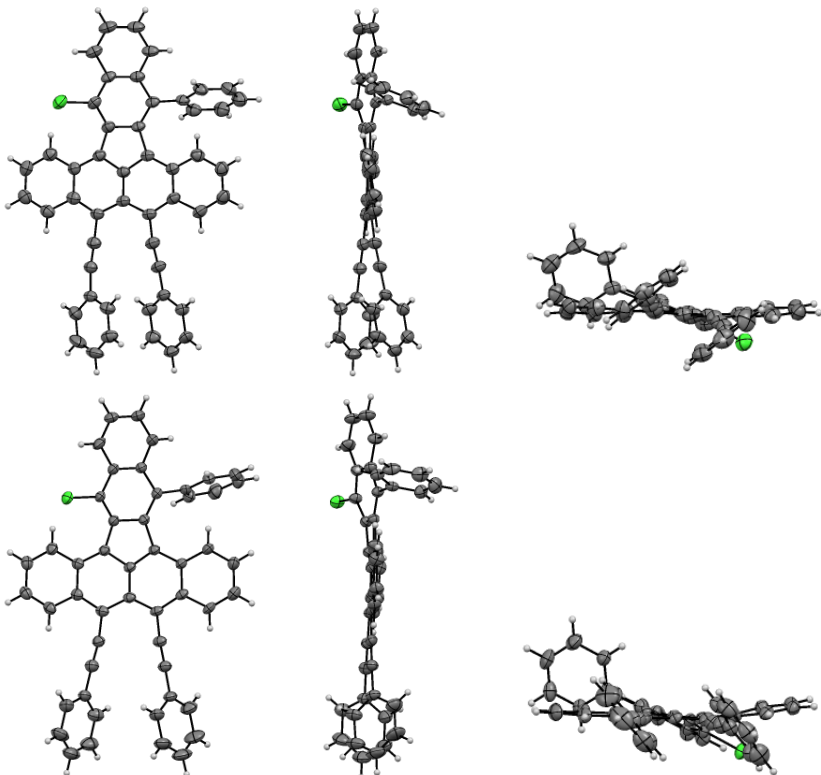


Figure S4. ORTEP drawings of **11a** (top: Mol-A, bottom: Mol-B) at the 50% probability level (CCDC 1871071).

$C_{50}H_{27}Cl$, MW = 663.16, 0.55 x 0.10 x 0.08 mm, Triclinic, space group $P\bar{1}$, $Z = 4$, $T = 200(2)$ K, $a = 10.264(5)$ Å, $b = 14.861(8)$ Å, $c = 24.721(11)$ Å, $\alpha = 92.409(6)^\circ$, $\beta = 91.727(7)^\circ$, $\gamma = 104.223(7)^\circ$, $V =$

$3649(3)$ Å³, $\lambda(\text{Mo K}\alpha) = 0.71075$ Å, $\mu = 0.139$ mm⁻¹. Intensity data were collected on a Rigaku R-AXIS RAPID II. The structure was solved by direct methods (*SHELXS97*) and refined by the full-matrix least-squares on F^2 (*SHELXL-2014/7*). A total of 42434 reflections were measured and 16719 were independent. Final $R_1 = 0.0666$, $wR_2 = 0.2024$ (11364 refs; $I > 2\sigma(I)$), and GOF = 1.070 (for all data, $R_1 = 0.0945$, $wR_2 = 0.2493$).

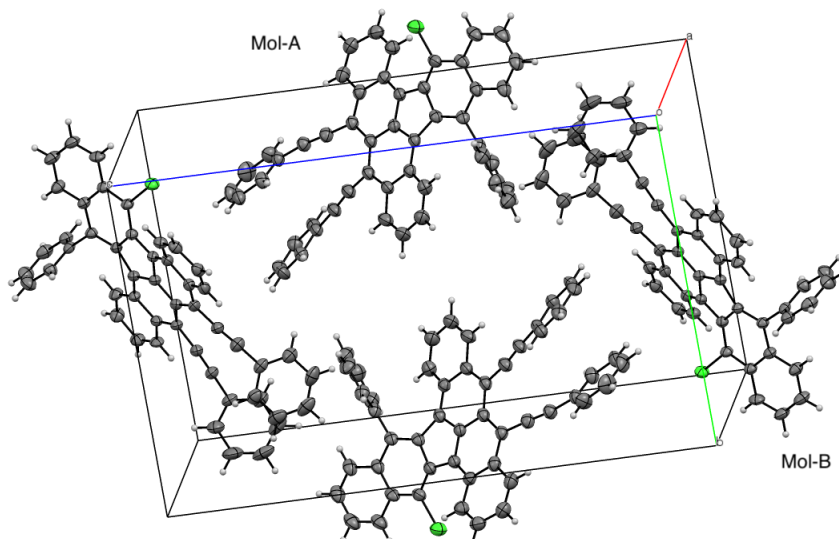


Figure S5. Packing structure of **11a** at the 50% probability level (CCDC 1871071).

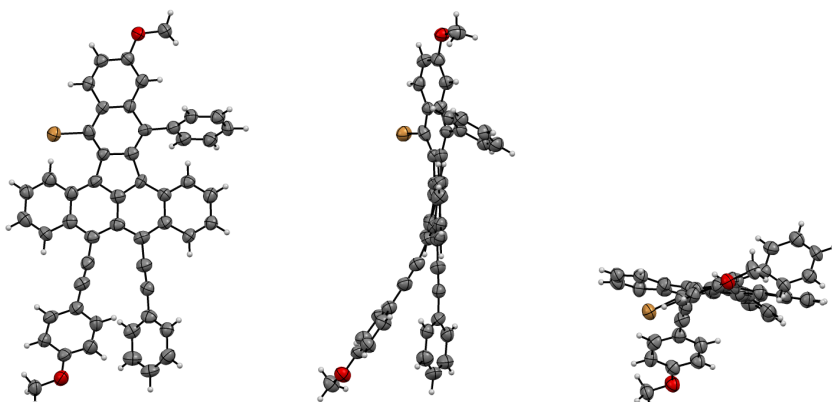
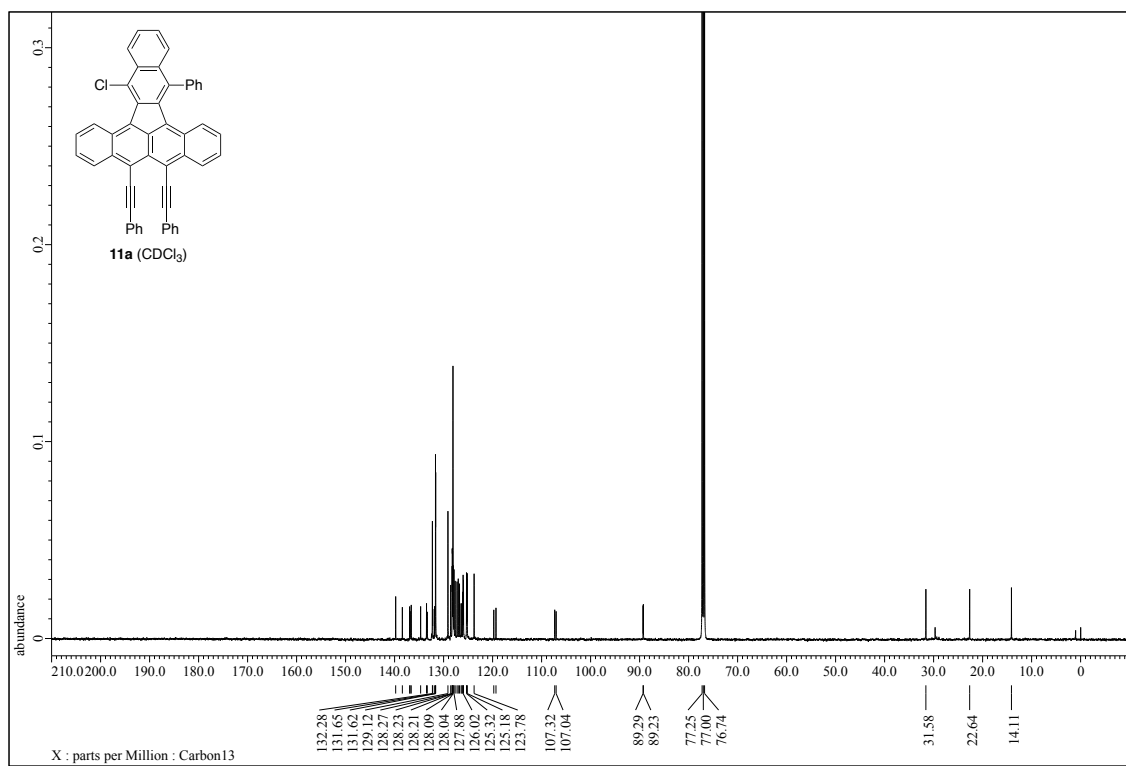
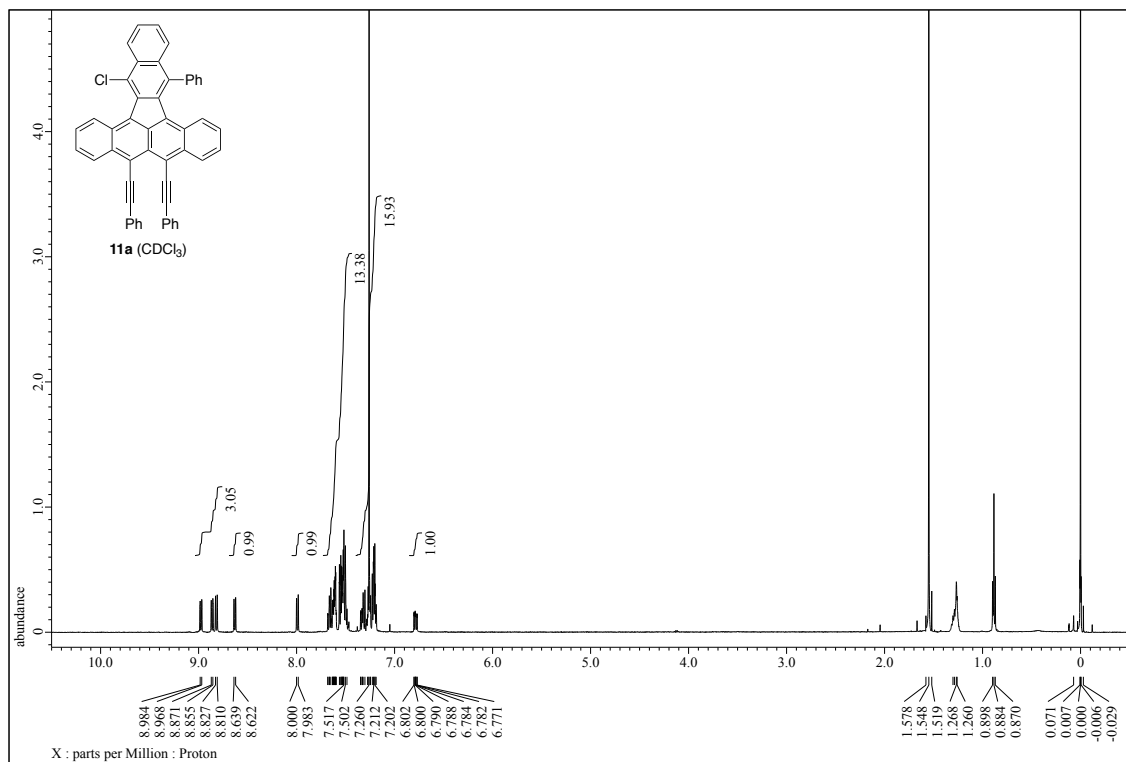
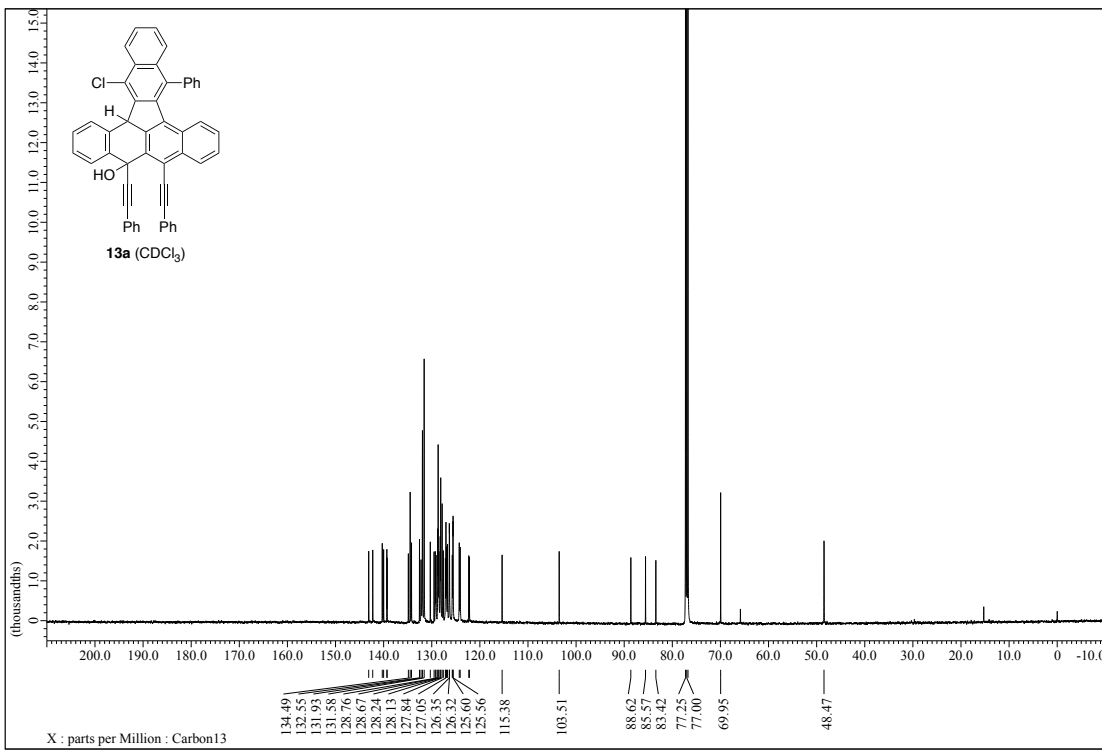
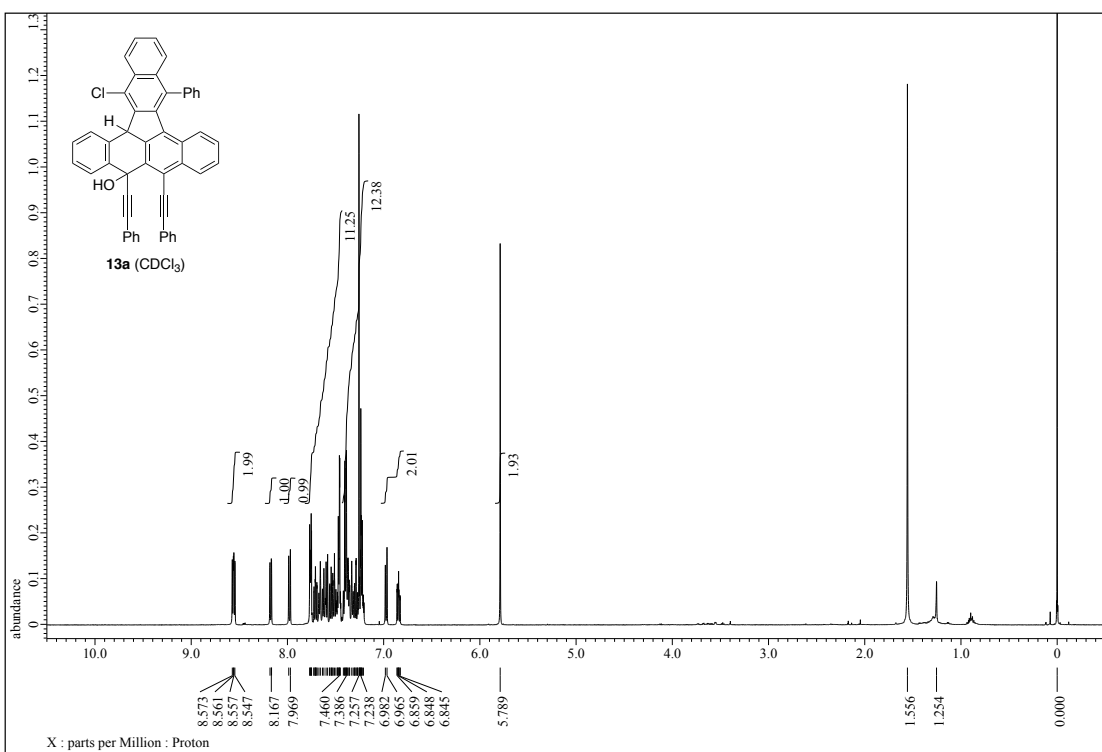


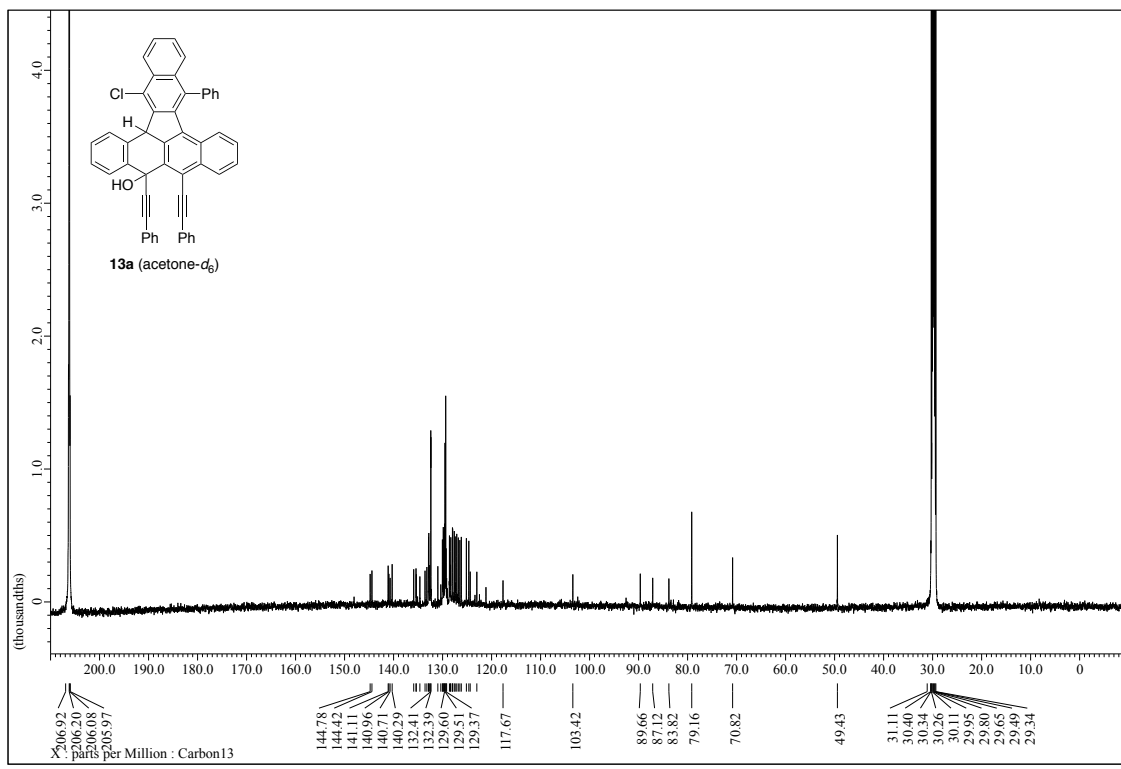
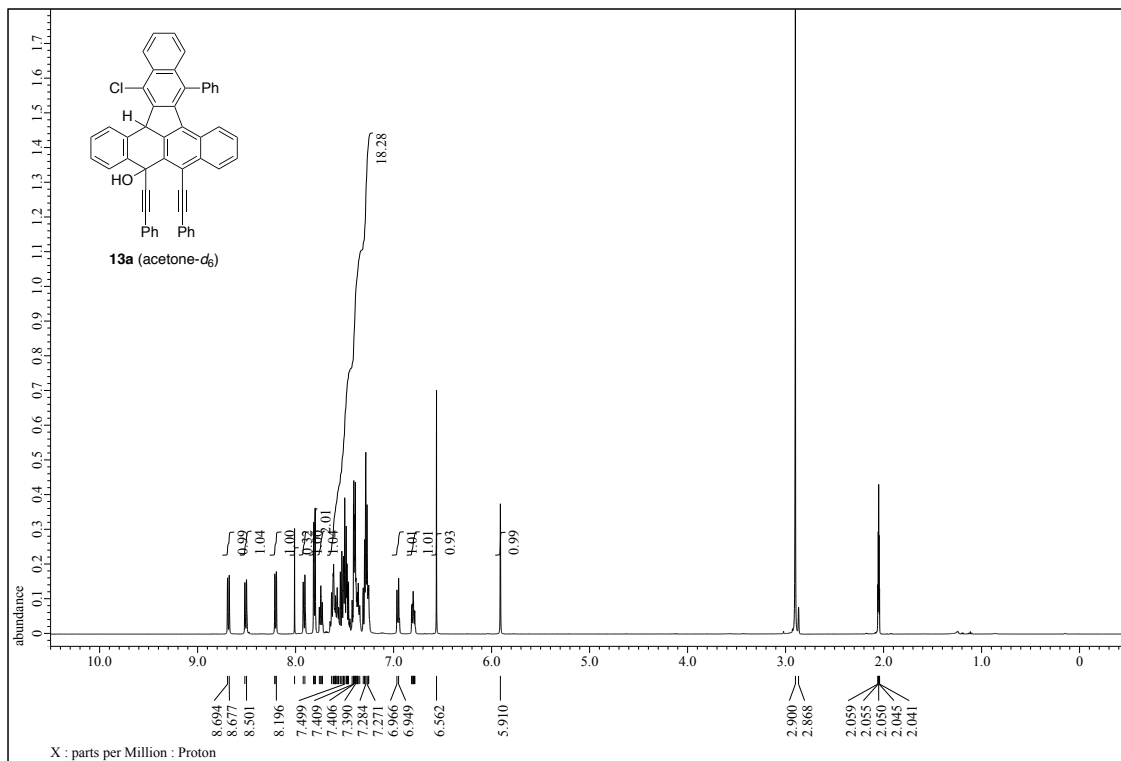
Figure S5. ORTEP drawings of **8a** at the 50% probability level (CCDC 1871070). The solvent molecule (C₆H₆) is omitted for clarity.

C₅₂H₃₁BrO₂·C₆H₆, MW = 845.78, 0.122 x 0.010 x 0.010 mm, Triclinic, space group *P*−1, $Z = 2$, T = 93(2) K, $a = 10.0716(3)$ Å, $b = 12.9698(4)$ Å, $c = 15.7503(4)$ Å, $\alpha = 91.289(2)^\circ$, $\beta = 95.8040(10)^\circ$, $\gamma = 90.059(2)^\circ$, $V = 12046.33(10)$ Å³, $\lambda(\text{Cu K}\alpha) = 1.54186$ Å, $\mu = 1.725$ mm⁻¹. Intensity data were collected on a Rigaku R-AXIS RAPID II. The structure was solved by direct methods (*SHELXS97*) and refined by the full-matrix least-squares on F^2 (*SHELXL-2014/7*). A total of 23945 reflections were measured and 7346 were independent. Final $R_1 = 0.1076$, $wR_2 = 0.2301$ (2651 refs; $I > 2\sigma(I)$), and GOF = 0.916 (for all data, $R_1 = 0.2000$, $wR_2 = 0.3081$).

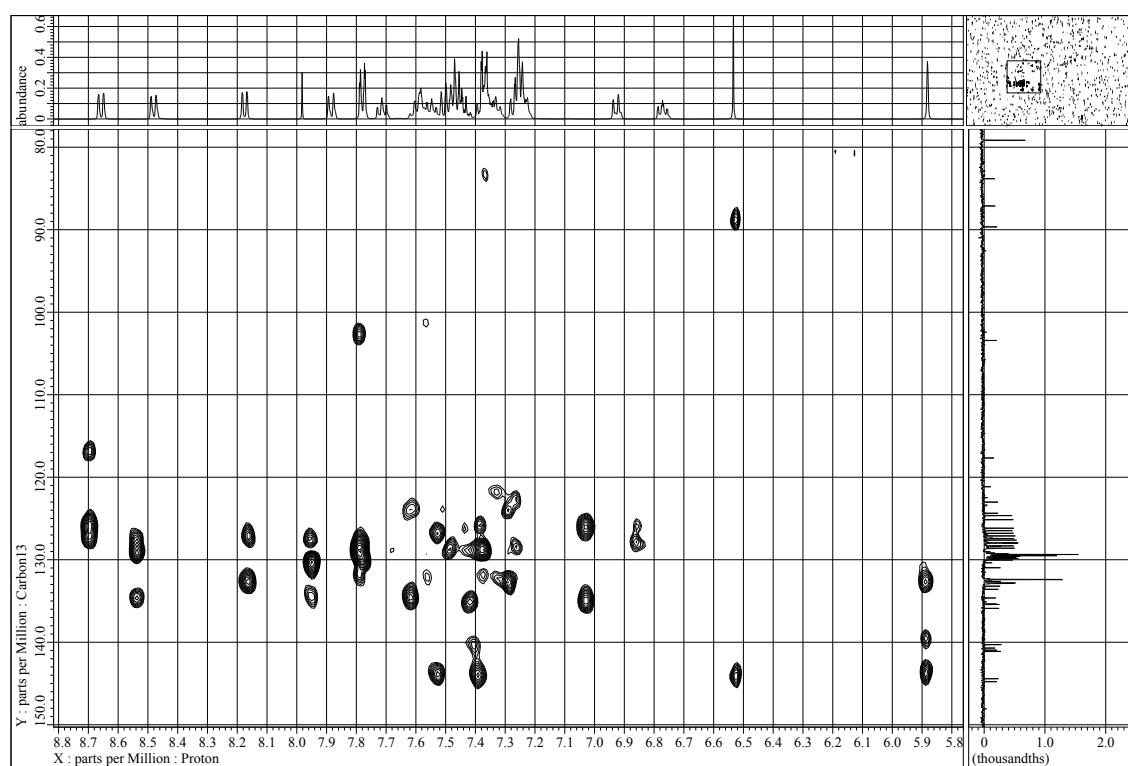
10. NMR spectra

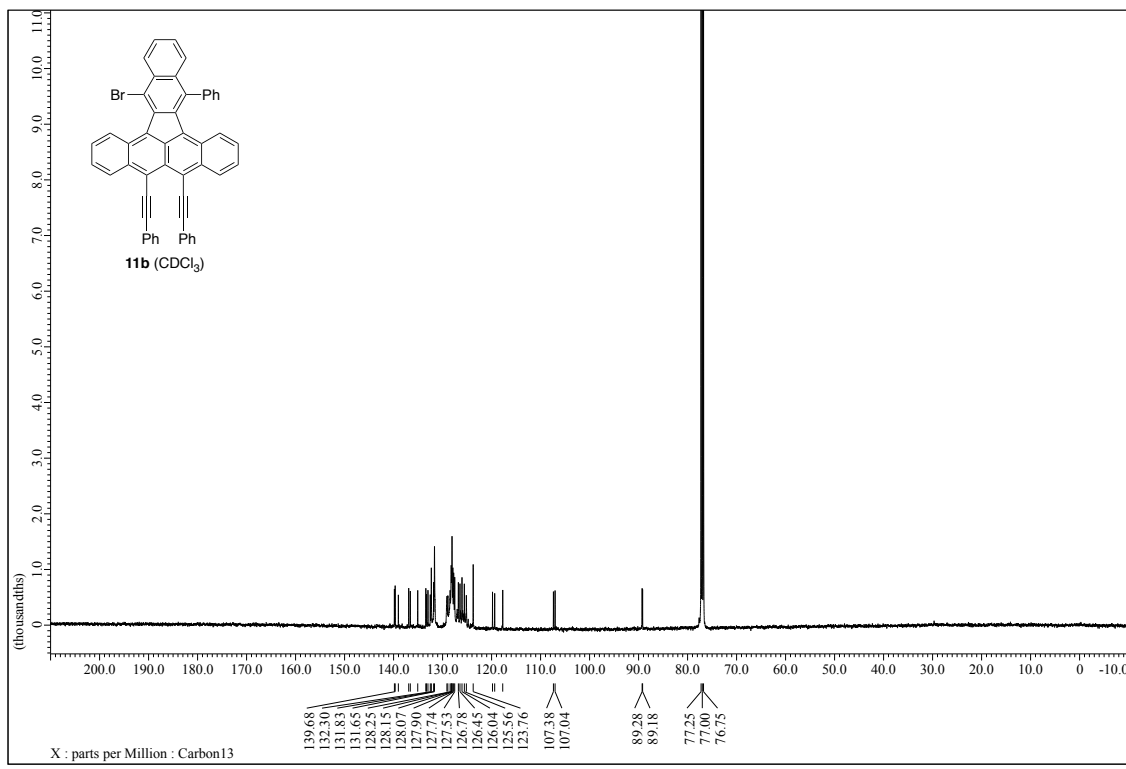
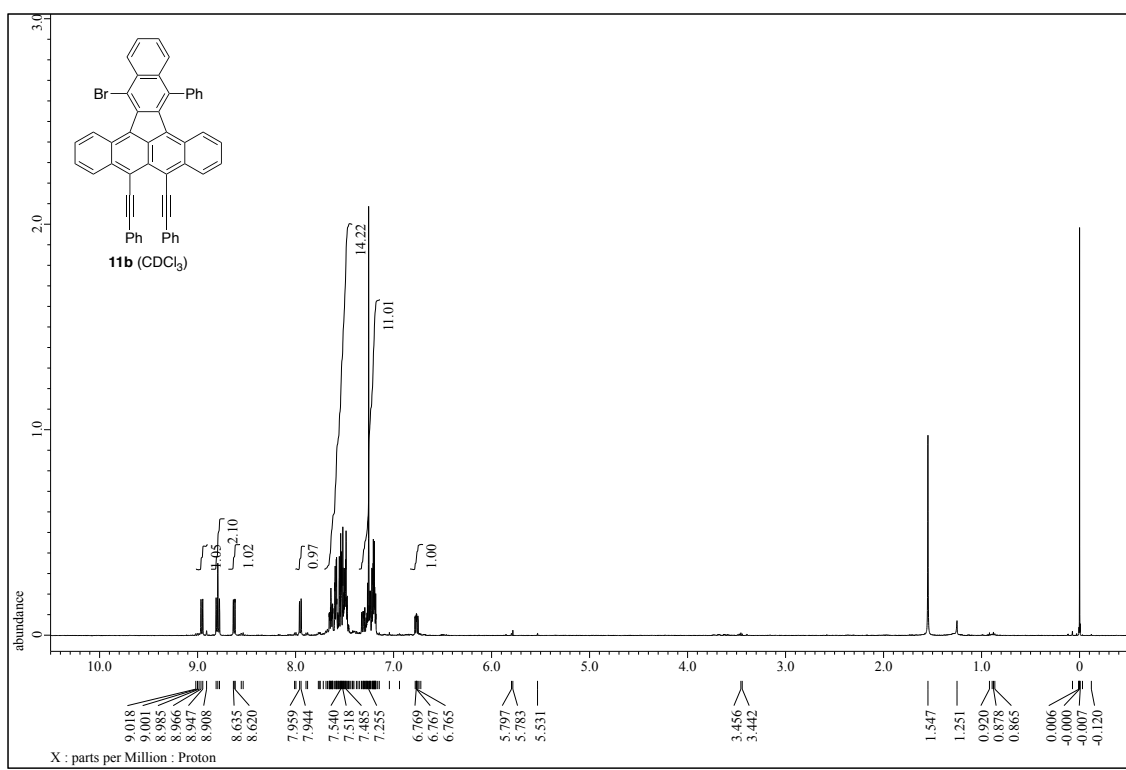


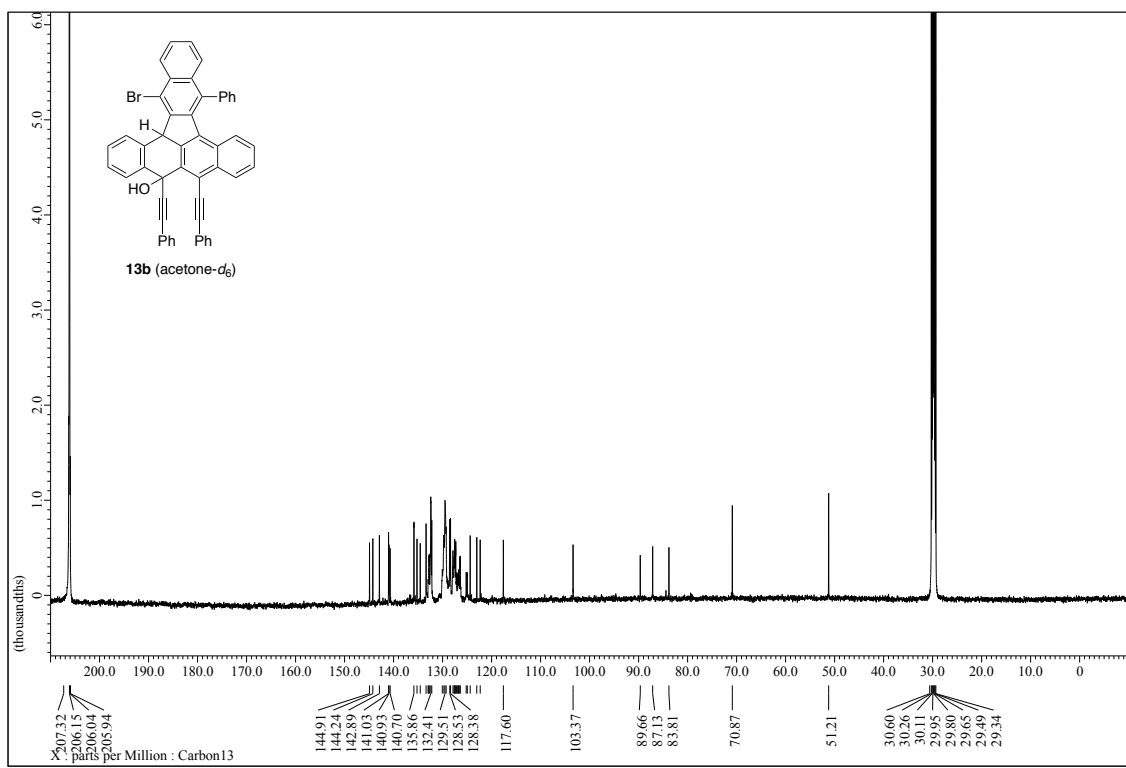
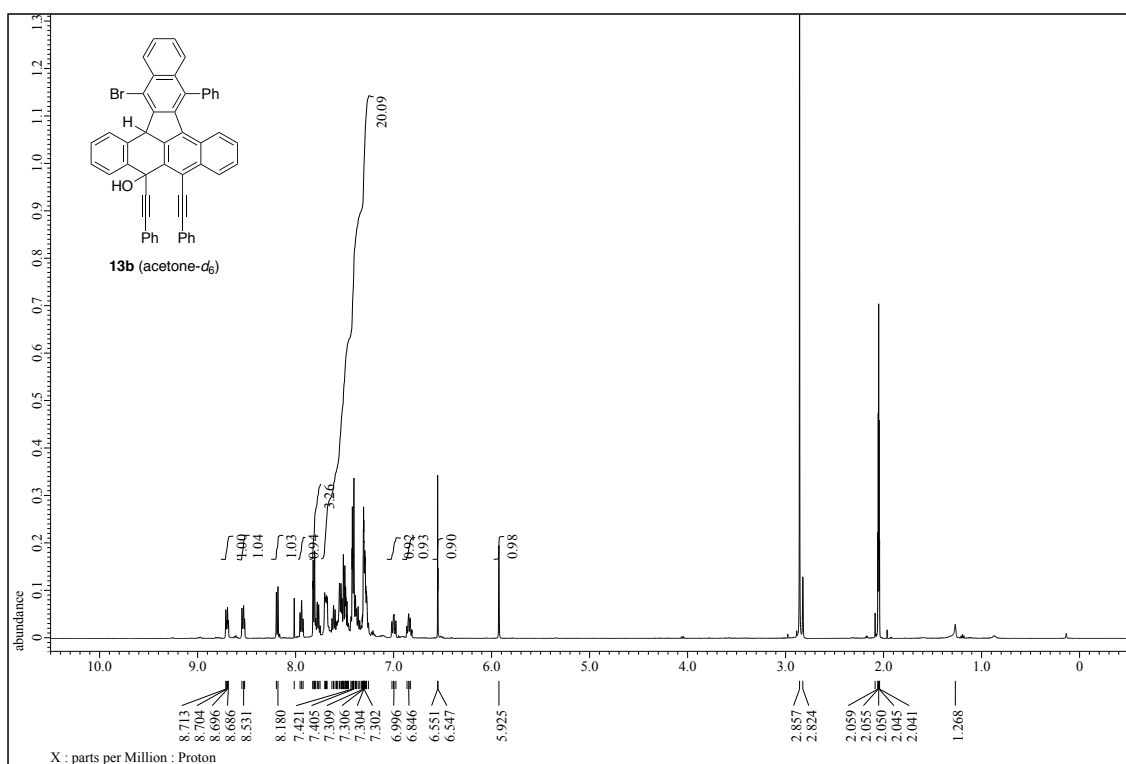




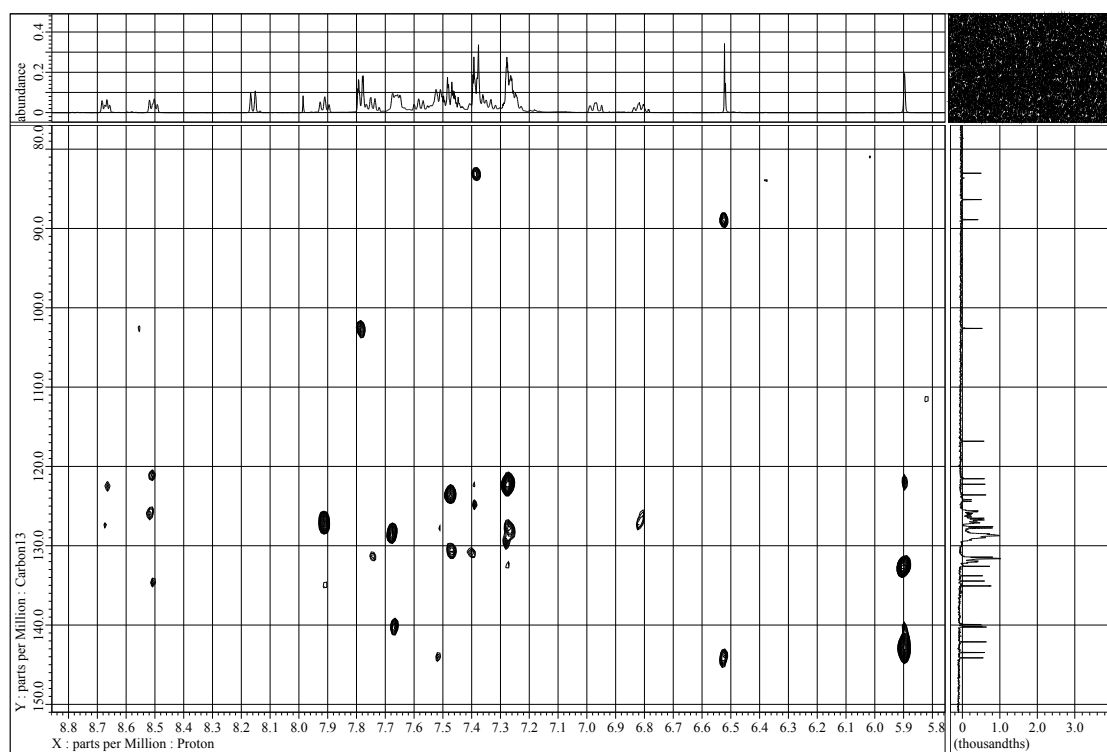
2D-NMR spectra (HMBC) of compound **13a** in acetone-*d*₆

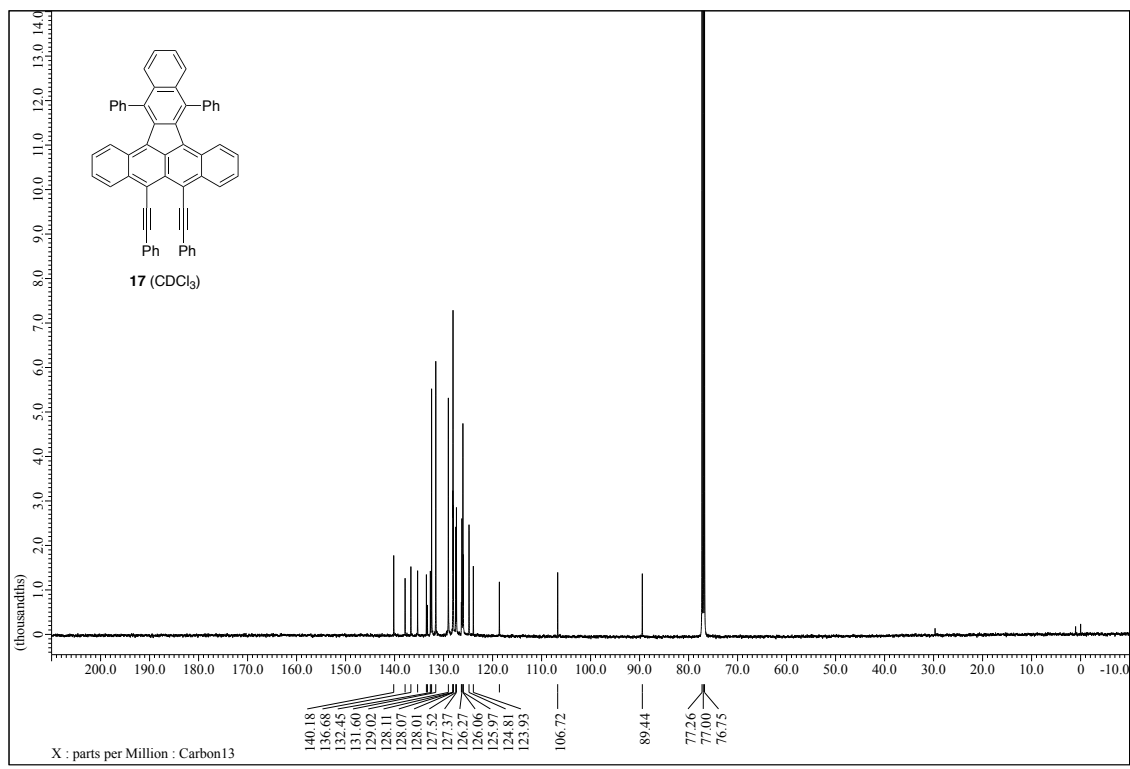
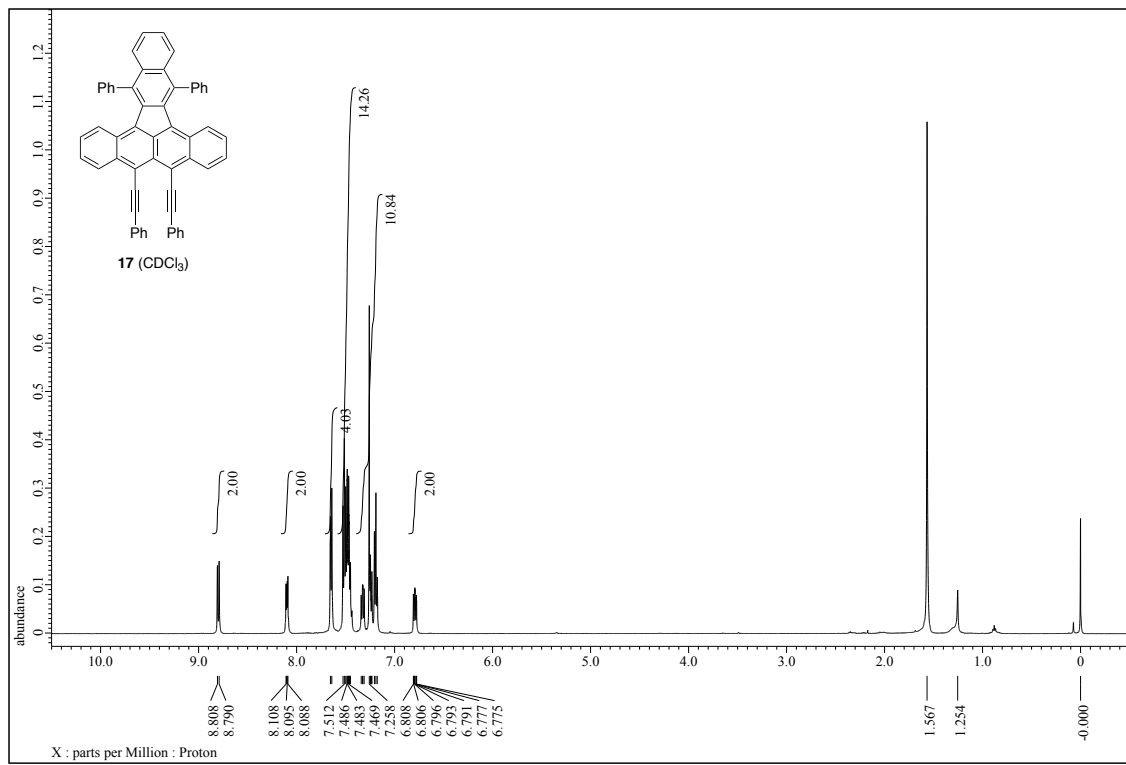


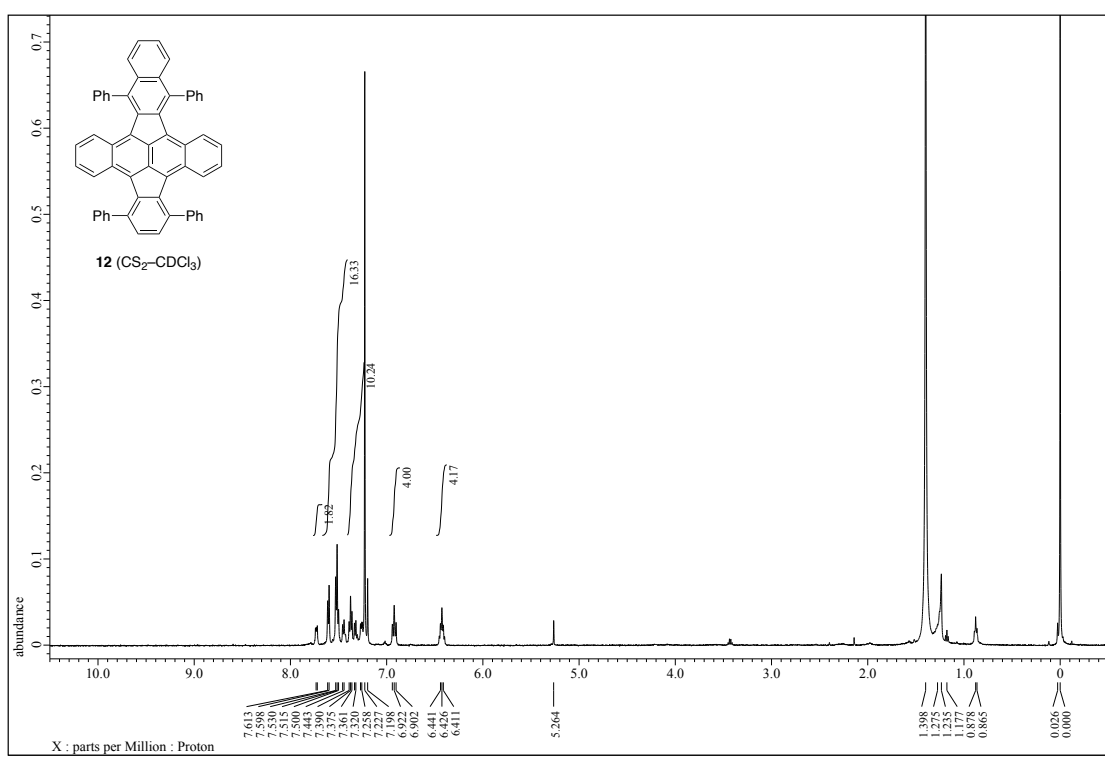


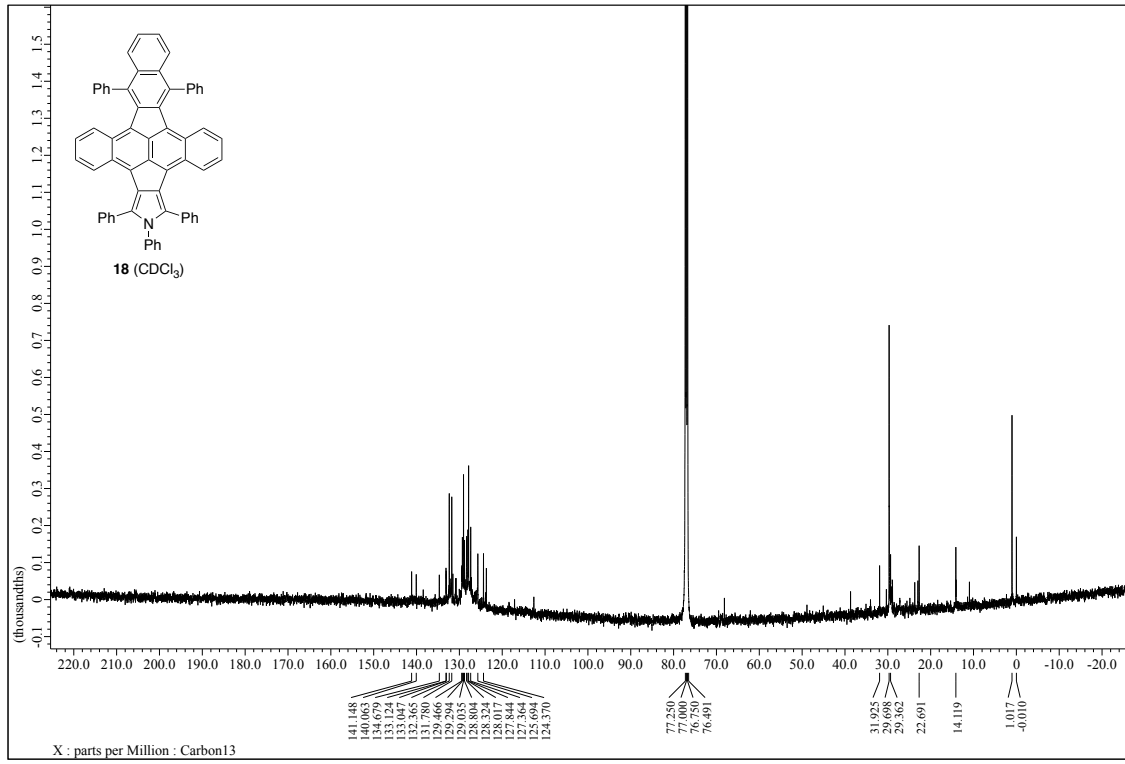
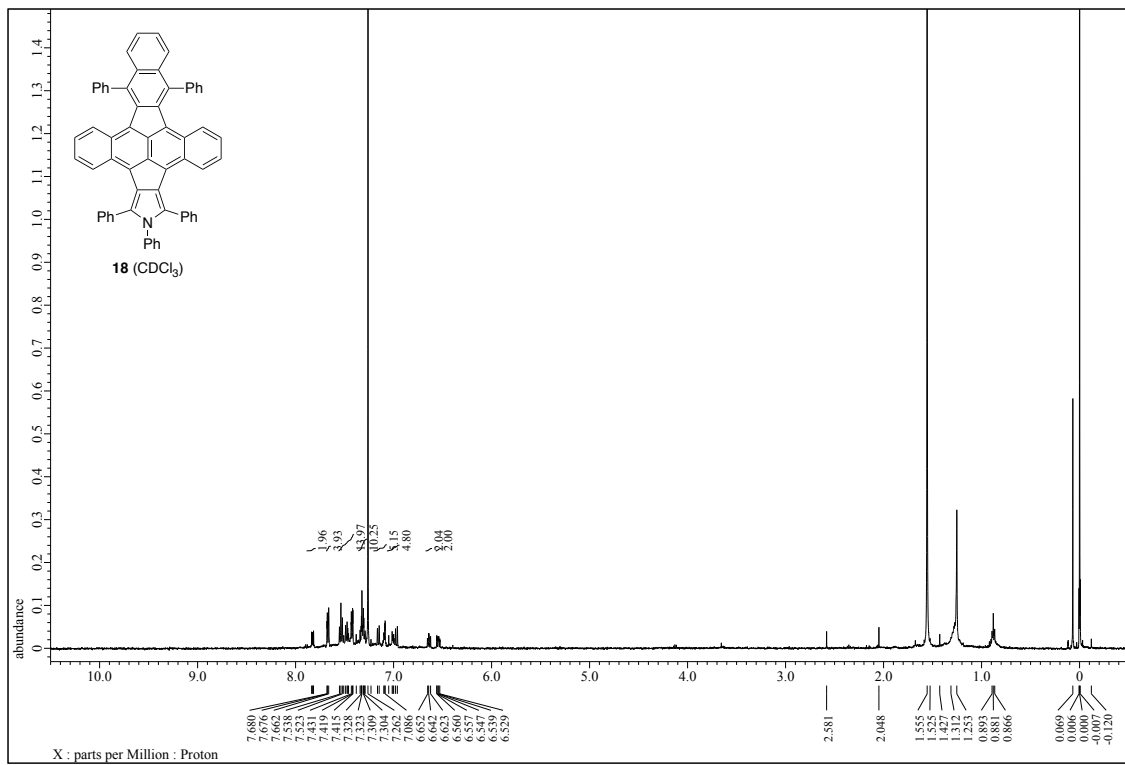


2D-NMR spectra (HMBC) of compound **13b** in acetone-*d*₆









11. Theoretical calculations

DFT calculations were performed with the Gaussian 09 program^[S2]. All geometry optimizations were carried out at the RB3LYP level of density functional theory with the 6-31G* basis set. Optical transitions with oscillator strength were calculated at the TD-B3LYP/6-31G* level using the optimized structures at the B3LYP/6-31G* level. NICS(0) values were calculated at the GIAO-B3LYP/6-31G* level using the optimized structures at the B3LYP/6-31G* level.

TD-DFT calculations

Table S1. Selected electronic transitions of **17** calculated at the TD-B3LYP/6-31G* level.

excited state	energy (eV)	wavelength (nm)	oscillator strengths (<i>f</i>)	contributed MOs	
1	1.7681	701.21	0.4682	0.70773	(HOMO → LUMO)
2	2.3781	521.35	0.0000	0.70325	(HOMO–2 → LUMO)
3	2.3909	518.57	0.0075	0.69679	(HOMO–1 → LUMO)

Table S2. Selected electronic transitions of **12** calculated at the TD-B3LYP/6-31G* level.

excited state	energy (eV)	wavelength (nm)	oscillator strengths (<i>f</i>)	contributed MOs	
1	1.7438	710.98	0.3999	0.70664	(HOMO → LUMO)
2	1.9122	648.37	0.0010	0.70577	(HOMO–1 → LUMO)
3	2.7837	445.39	0.0354	0.69136 -0.10437	(HOMO–2 → LUMO) (HOMO–1 → LUMO+1)

Table S3. Selected electronic transitions of **18** calculated at the TD-B3LYP/6-31G* level.

excited state	energy (eV)	wavelength (nm)	oscillator strengths (<i>f</i>)	contributed MOs	
1	1.7678	701.34	0.4472	0.70665	(HOMO → LUMO)
2	1.9471	636.76	0.0015	0.70494	(HOMO–1 → LUMO)
3	2.8472	435.46	0.0036	0.10820 0.69148	(HOMO–5 → LUMO) (HOMO → LUMO+1)

NICS calculations

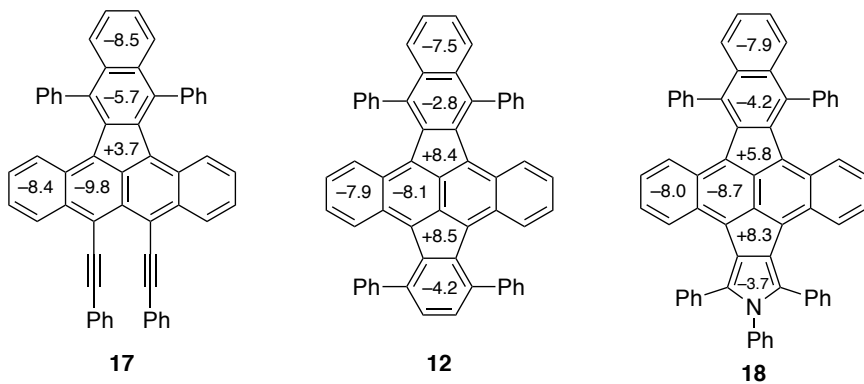


Figure S6. NICS(0) values for compounds **17**, **12**, and **18** calculated at the GIAO-B3LYP/6-31G*

Optimized Geometries

compound 17 (B3LYP/6-31G*)

Center Number	Atomic Number	Atomic Type	Coordinates (Angstroms)		
			X	Y	Z
1	6	0	0.000000	2.455729	0.920214
2	6	0	0.000000	1.255936	1.678064
3	6	0	0.000000	0.000000	1.007403
4	6	0	0.000000	0.000000	-0.427874
5	6	0	0.000000	1.185815	-1.217276
6	6	0	0.000000	2.440516	-0.535535
7	6	0	0.000000	-1.255936	1.678064
8	6	0	0.000000	-1.185815	-1.217276
9	6	0	0.000000	-2.440516	-0.535535
10	6	0	0.000000	-2.455729	0.920214
11	6	0	0.000000	-3.710775	1.611643
12	1	0	0.000000	-3.691525	2.693154
13	6	0	0.000000	-4.906724	0.953018
14	6	0	0.000000	-4.906800	-0.461721
15	6	0	0.000000	-3.726983	-1.156790
16	1	0	0.000000	-5.840844	1.508092
17	1	0	0.000000	-5.843888	-1.011643
18	1	0	0.000000	-3.783777	-2.221313
19	6	0	0.000000	3.726983	-1.156790
20	6	0	0.000000	4.906800	-0.461721
21	1	0	0.000000	5.843888	-1.011643
22	6	0	0.000000	4.906724	0.953018
23	1	0	0.000000	5.840844	1.508092
24	6	0	0.000000	3.710775	1.611643
25	1	0	0.000000	3.691525	2.693154
26	6	0	0.000000	-0.739599	-2.646211
27	6	0	0.000000	0.739599	-2.646211
28	6	0	0.000000	-1.431562	-3.861677
29	6	0	0.000000	-0.711647	-5.109282
30	6	0	0.000000	0.711647	-5.109282
31	6	0	0.000000	1.431562	-3.861677
32	6	0	0.000000	-1.388121	-6.366059
33	6	0	0.000000	-0.703951	-7.560093
34	1	0	0.000000	-1.253277	-8.497723
35	6	0	0.000000	0.703951	-7.560093
36	1	0	0.000000	1.253277	-8.497723
37	6	0	0.000000	1.388121	-6.366059
38	1	0	0.000000	2.468833	-6.388874
39	1	0	0.000000	3.783777	-2.221313
40	1	0	0.000000	-2.468833	-6.388874
41	6	0	0.000000	-1.376486	3.098473

42	6	0	0.000000	1.376486	3.098473
43	6	0	0.000000	-1.679000	4.278489
44	6	0	0.000000	1.679000	4.278489
45	6	0	0.000000	-1.987038	5.671428
46	6	0	1.213202	-2.151075	6.369205
47	6	0	-1.213202	-2.151075	6.369205
48	6	0	1.208267	-2.467587	7.724995
49	1	0	2.150274	-2.026802	5.835323
50	6	0	-1.208267	-2.467587	7.724995
51	1	0	-2.150274	-2.026802	5.835323
52	6	0	0.000000	-2.627495	8.407563
53	1	0	2.151283	-2.590388	8.251023
54	1	0	-2.151283	-2.590388	8.251023
55	1	0	0.000000	-2.875310	9.465553
56	6	0	0.000000	1.987038	5.671428
57	6	0	1.213202	2.151075	6.369205
58	6	0	-1.213202	2.151075	6.369205
59	6	0	1.208267	2.467587	7.724995
60	1	0	2.150274	2.026802	5.835323
61	6	0	-1.208267	2.467587	7.724995
62	1	0	-2.150274	2.026802	5.835323
63	6	0	0.000000	2.627495	8.407563
64	1	0	2.151283	2.590388	8.251023
65	1	0	-2.151283	2.590388	8.251023
66	1	0	0.000000	2.875310	9.465553
67	6	0	0.000000	-2.913850	-4.074810
68	6	0	-1.207484	-3.605408	-4.253784
69	6	0	1.207484	-3.605408	-4.253784
70	6	0	-1.207721	-4.968855	-4.550354
71	1	0	-2.146788	-3.070822	-4.142939
72	6	0	1.207721	-4.968855	-4.550354
73	1	0	2.146788	-3.070822	-4.142939
74	6	0	0.000000	-5.656266	-4.693684
75	1	0	-2.151497	-5.494016	-4.671679
76	1	0	2.151497	-5.494016	-4.671679
77	1	0	0.000000	-6.718169	-4.924555
78	6	0	0.000000	2.913850	-4.074810
79	6	0	-1.207484	3.605408	-4.253784
80	6	0	1.207484	3.605408	-4.253784
81	6	0	-1.207721	4.968855	-4.550354
82	1	0	-2.146788	3.070822	-4.142939
83	6	0	1.207721	4.968855	-4.550354
84	1	0	2.146788	3.070822	-4.142939
85	6	0	0.000000	5.656266	-4.693684
86	1	0	-2.151497	5.494016	-4.671679
87	1	0	2.151497	5.494016	-4.671679
88	1	0	0.000000	6.718169	-4.924555

compound **12** (B3LYP/6-31G*)

Center Number	Atomic Number	Atomic Type	Coordinates (Angstroms)		
			X	Y	Z
1	6	0	0.000000	4.868205	1.201682
2	6	0	0.000000	3.669235	1.859376
3	6	0	0.000000	2.404177	1.200862
4	6	0	0.000000	2.412834	-0.279048
5	6	0	0.000000	3.698395	-0.898084
6	6	0	0.000000	4.881242	-0.209688
7	6	0	0.000000	1.178850	1.918658
8	6	0	0.000000	1.188580	-1.014673
9	6	0	0.000000	0.000000	-0.253514
10	6	0	0.000000	0.000000	1.150583
11	6	0	0.000000	-1.178850	1.918658
12	6	0	0.000000	-2.404177	1.200862
13	6	0	0.000000	-2.412834	-0.279048
14	6	0	0.000000	-1.188580	-1.014673
15	1	0	0.000000	5.794998	1.768887
16	1	0	0.000000	3.678075	2.929698
17	1	0	0.000000	3.743944	-1.964493
18	1	0	0.000000	5.819261	-0.757937
19	6	0	0.000000	-3.698395	-0.898084
20	6	0	0.000000	-4.881242	-0.209688
21	1	0	0.000000	-5.819261	-0.757937
22	6	0	0.000000	-4.868205	1.201682
23	1	0	0.000000	-5.794998	1.768887
24	6	0	0.000000	-3.669235	1.859376
25	1	0	0.000000	-3.678075	2.929698
26	6	0	0.000000	0.742724	-2.449333
27	6	0	0.000000	-0.742724	-2.449333
28	6	0	0.000000	0.732151	3.346828
29	6	0	0.000000	-0.732151	3.346828
30	6	0	0.000000	1.432898	-3.660179
31	6	0	0.000000	0.711352	-4.910893
32	6	0	0.000000	-0.711352	-4.910893
33	6	0	0.000000	-1.432898	-3.660179
34	6	0	0.000000	1.388221	-6.164370
35	6	0	0.000000	0.703172	-7.360047
36	1	0	0.000000	1.252635	-8.297585
37	6	0	0.000000	-0.703172	-7.360047
38	1	0	0.000000	-1.252635	-8.297585
39	6	0	0.000000	-1.388221	-6.164370
40	1	0	0.000000	-2.469347	-6.185101
41	6	0	0.000000	1.428554	4.577418
42	6	0	0.000000	0.688552	5.770857
43	1	0	0.000000	1.226479	6.713930

44	6	0	0.000000	-0.688552	5.770857
45	1	0	0.000000	-1.226479	6.713930
46	6	0	0.000000	-1.428554	4.577418
47	1	0	0.000000	2.469347	-6.185101
48	1	0	0.000000	-3.743944	-1.964493
49	6	0	0.000000	2.916988	-3.859376
50	6	0	-1.207488	3.611452	-4.026259
51	6	0	1.207488	3.611452	-4.026259
52	6	0	-1.207661	4.979309	-4.301803
53	1	0	-2.146913	3.075653	-3.922416
54	6	0	1.207661	4.979309	-4.301803
55	1	0	2.146913	3.075653	-3.922416
56	6	0	0.000000	5.668669	-4.434966
57	1	0	-2.151461	5.506414	-4.414089
58	1	0	2.151461	5.506414	-4.414089
59	1	0	0.000000	6.734037	-4.649299
60	6	0	0.000000	-2.916988	-3.859376
61	6	0	-1.207488	-3.611452	-4.026259
62	6	0	1.207488	-3.611452	-4.026259
63	6	0	-1.207661	-4.979309	-4.301803
64	1	0	-2.146913	-3.075653	-3.922416
65	6	0	1.207661	-4.979309	-4.301803
66	1	0	2.146913	-3.075653	-3.922416
67	6	0	0.000000	-5.668669	-4.434966
68	1	0	-2.151461	-5.506414	-4.414089
69	1	0	2.151461	-5.506414	-4.414089
70	1	0	0.000000	-6.734037	-4.649299
71	6	0	0.000000	2.902271	4.860059
72	6	0	1.207031	3.583367	5.078856
73	6	0	-1.207031	3.583367	5.078856
74	6	0	1.206962	4.925738	5.459900
75	1	0	2.146970	3.058135	4.933164
76	6	0	-1.206962	4.925738	5.459900
77	1	0	-2.146970	3.058135	4.933164
78	6	0	0.000000	5.602628	5.647433
79	1	0	2.151075	5.441664	5.614503
80	1	0	-2.151075	5.441664	5.614503
81	1	0	0.000000	6.647854	5.944949
82	6	0	0.000000	-2.902271	4.860059
83	6	0	1.207031	-3.583367	5.078856
84	6	0	-1.207031	-3.583367	5.078856
85	6	0	1.206962	-4.925738	5.459900
86	1	0	2.146970	-3.058135	4.933164
87	6	0	-1.206962	-4.925738	5.459900
88	1	0	-2.146970	-3.058135	4.933164
89	6	0	0.000000	-5.602628	5.647433
90	1	0	2.151075	-5.441664	5.614503
91	1	0	-2.151075	-5.441664	5.614503

92 1 0 0.000000 -6.647854 5.944949

compound 18 (B3LYP/6-31G*)

Center Number	Atomic Number	Atomic Type	Coordinates (Angstroms)		
			X	Y	Z
1	6	0	0.000000	4.859819	0.504494
2	6	0	0.000000	3.650717	1.141923
3	6	0	0.000000	2.407775	0.437836
4	6	0	0.000000	2.423250	-1.040752
5	6	0	0.000000	3.723748	-1.630757
6	6	0	0.000000	4.889217	-0.909601
7	6	0	0.000000	1.184093	1.135166
8	6	0	0.000000	1.196098	-1.783056
9	6	0	0.000000	0.000000	-1.028813
10	6	0	0.000000	0.000000	0.369214
11	6	0	0.000000	-1.184093	1.135166
12	6	0	0.000000	-2.407775	0.437836
13	6	0	0.000000	-2.423250	-1.040752
14	6	0	0.000000	-1.196098	-1.783056
15	1	0	0.000000	5.781982	1.079300
16	1	0	0.000000	3.619255	2.218796
17	1	0	0.000000	3.800728	-2.696594
18	1	0	0.000000	5.838303	-1.438970
19	6	0	0.000000	-3.723748	-1.630757
20	6	0	0.000000	-4.889217	-0.909601
21	1	0	0.000000	-5.838303	-1.438970
22	6	0	0.000000	-4.859819	0.504494
23	1	0	0.000000	-5.781982	1.079300
24	6	0	0.000000	-3.650717	1.141923
25	1	0	0.000000	-3.619255	2.218796
26	6	0	0.000000	-0.743942	-3.212243
27	6	0	0.000000	0.743942	-3.212243
28	6	0	0.000000	0.722140	2.537551
29	6	0	0.000000	-0.722140	2.537551
30	6	0	0.000000	1.432318	-4.424421
31	6	0	0.000000	0.712164	-5.673097
32	6	0	0.000000	-0.712164	-5.673097
33	6	0	0.000000	-1.432318	-4.424421
34	6	0	0.000000	1.148287	3.848439
35	6	0	0.000000	1.388931	-6.927353
36	6	0	0.000000	0.703778	-8.122307
37	1	0	0.000000	1.252637	-9.060312
38	6	0	0.000000	-0.703778	-8.122307
39	1	0	0.000000	-1.252637	-9.060312
40	6	0	0.000000	-1.388931	-6.927353

41	1	0	0.000000	-2.470447	-6.946764
42	1	0	0.000000	2.470447	-6.946764
43	1	0	0.000000	-3.800728	-2.696594
44	6	0	0.000000	-1.148287	3.848439
45	6	0	0.000000	2.564056	4.298301
46	6	0	1.209011	3.255931	4.473917
47	6	0	-1.209011	3.255931	4.473917
48	6	0	1.208437	4.604090	4.832287
49	1	0	2.147388	2.729679	4.325428
50	6	0	-1.208437	4.604090	4.832287
51	1	0	-2.147388	2.729679	4.325428
52	6	0	0.000000	5.280750	5.014810
53	1	0	2.151632	5.127639	4.963111
54	1	0	-2.151632	5.127639	4.963111
55	1	0	0.000000	6.331376	5.292355
56	6	0	0.000000	-2.564056	4.298301
57	6	0	-1.209011	-3.255931	4.473917
58	6	0	1.209011	-3.255931	4.473917
59	6	0	-1.208437	-4.604090	4.832287
60	1	0	-2.147388	-2.729679	4.325428
61	6	0	1.208437	-4.604090	4.832287
62	1	0	2.147388	-2.729679	4.325428
63	6	0	0.000000	-5.280750	5.014810
64	1	0	-2.151632	-5.127639	4.963111
65	1	0	2.151632	-5.127639	4.963111
66	1	0	0.000000	-6.331376	5.292355
67	6	0	0.000000	2.917517	-4.609691
68	6	0	-1.207173	3.614853	-4.766315
69	6	0	1.207173	3.614853	-4.766315
70	6	0	-1.207626	4.986422	-5.023284
71	1	0	-2.146495	3.077493	-4.669733
72	6	0	1.207626	4.986422	-5.023284
73	1	0	2.146495	3.077493	-4.669733
74	6	0	0.000000	5.677623	-5.146913
75	1	0	-2.151456	5.515152	-5.128095
76	1	0	2.151456	5.515152	-5.128095
77	1	0	0.000000	6.745899	-5.346655
78	6	0	0.000000	-2.917517	-4.609691
79	6	0	1.207173	-3.614853	-4.766315
80	6	0	-1.207173	-3.614853	-4.766315
81	6	0	1.207626	-4.986422	-5.023284
82	1	0	2.146495	-3.077493	-4.669733
83	6	0	-1.207626	-4.986422	-5.023284
84	1	0	-2.146495	-3.077493	-4.669733
85	6	0	0.000000	-5.677623	-5.146913
86	1	0	2.151456	-5.515152	-5.128095
87	1	0	-2.151456	-5.515152	-5.128095
88	1	0	0.000000	-6.745899	-5.346655

89	6	0	0.000000	0.000000	6.138725
90	6	0	0.000000	-1.195153	6.885510
91	6	0	0.000000	1.195153	6.885510
92	6	0	0.000000	-1.190048	8.279531
93	1	0	0.000000	-2.154346	6.405778
94	6	0	0.000000	1.190048	8.279531
95	1	0	0.000000	2.154346	6.405778
96	6	0	0.000000	0.000000	8.999920
97	1	0	0.000000	-2.146129	8.796483
98	1	0	0.000000	2.146129	8.796483
99	1	0	0.000000	0.000000	10.086019
100	7	0	0.000000	0.000000	4.690157

12. References

- [S1] Kitamura, K.; Asahina, K.; Nagai, Y.; Sugiyama, H.; Uekusa, H.; Hamura, T. *Chem. Eur. J.* **2018**, *24*, 14034.
- [S2] Gaussian 09, Revision C.01, Frisch, M. J.; Trucks, G. W.; Schlegel, H. B.; Scuseria, G. E.; Robb, M. A.; Cheeseman, J. R.; Scalmani, G.; Barone, V.; Mennucci, B.; Petersson, G. A.; Nakatsuji, H.; Caricato, M.; Li, X.; Hratchian, H. P.; Izmaylov, A. F.; Bloino, J.; Zheng, G.; Sonnenberg, J. L.; Hada, M.; Ehara, M.; Toyota, K.; Fukuda, R.; Hasegawa, J.; Ishida, M.; Nakajima, T.; Honda, Y.; Kitao, O.; Nakai, H.; Vreven, T.; Montgomery, Jr., J. A.; Peralta, J. E.; Ogliaro, F.; Bearpark, M.; Heyd, J. J.; Brothers, E.; Kudin, K. N.; Staroverov, V. N.; Kobayashi, R.; Normand, J.; Raghavachari, K.; Rendell, A.; Burant, J. C.; Iyengar, S. S.; Tomasi, J.; Cossi, M.; Rega, N.; Millam, J. M.; Klene, M.; Knox, J. E.; Cross, J. B.; Bakken, V.; Adamo, C.; Jaramillo, J.; Gomperts, R.; Stratmann, R. E.; Yazyev, O.; Austin, A. J.; Cammi, R.; Pomelli, C.; Ochterski, J. W.; Martin, R. L.; Morokuma, K.; Zakrzewski, V. G.; Voth, G. A.; Salvador, P.; Dannenberg, J. J.; Dapprich, S.; Daniels, A. D.; Farkas, Ö.; Foresman, J. B.; Ortiz, J. V.; Cioslowski, J.; Fox, D. J. Gaussian, Inc., Wallingford CT, 2010.